Assessing the Performance of an Open Spatial Capture-Recapture Method on Grizzly Bear Populations When Age Data is Missing

by

Neil Faught

B.Sc., University of Guelph, 2016

Project Submitted in Partial Fulfillment of the
Requirements for the Degree of
Master of Science

in the
Department of Statistics and Actuarial Science
Faculty of Science

SIMON FRASER UNIVERSITY
Spring 2020

Approval

Name:	**Neil Faught**
Degree:	**Master of Science (Statistics)**
Title:	**Assessing the Performance of an Open Spatial Capture-Recapture Method on Grizzly Bear Populations When Age Data is Missing**
Examining Committee:	**Chair:** Jinko Graham Professor
	Steven Thompson Senior Supervisor Professor
	Carl Schwarz Supervisor Professor Emeritus
	Rick Routledge Internal Examiner Professor Emeritus
	Liangliang Wang External Examiner Associate Professor
Date Defended/Approved:	February 13th, 2020

Abstract

It is often difficult in capture-recapture (CR) studies of grizzly bear populations to determine the age of detected bears. As a result, analyses often omit age terms in CR models despite past studies suggesting age influences detection probability. This paper explores how failing to account for age in the detection function of an open, spatially-explicit CR model, introduced in Efford & Schofield (2019), affects estimates of apparent survival, apparent recruitment, population growth, and grizzly bear home-range sizes. Using a simulation study, it was found that estimates of all parameters of interest excluding home-range size were robust to this omission. The effects of using two different types of detectors for data collection (bait sites and rub objects) on bias in estimates of above parameters was also explored via simulation. No evidence was found that one detector type was more prone to producing biased parameter estimates than the other.

Keywords: capture-recapture; spatially explicit; open population; grizzly bear; simulation study; age data

Acknowledgements

Many people helped me complete this project. I would first and foremost like to thank my supervisors Steve Thompson and Carl Schwarz, for providing me with many opportunities to learn about statistical ecology, and for financial assistance throughout my degree. Your constant support and mentorship made this work possible and made me a much better statistician than I was when I first arrived at SFU.

Thank you to my committee members for taking the time to read and provide feedback on this paper.

Thank you to Garth Mowat, for letting me join him and his team during the 2019 South Rockies Grizzly Bear Project Fall sampling period, for comments on this paper's first draft, and for putting me up while I was in Nelson.

Thank you to Clayton Lamb and Laura Smit for answering the many questions I had about the South Rockies Grizzly Bear Project.

Special thanks to my friends and family for always supporting me. I have met so many wonderful people since arriving at SFU, too many to include in this short section alone; that said, I am especially grateful to Tory Frizzell and Joel Therrien, who were always by my side and helped with this project in more ways than they know.

Finally, I would like to thank Dr. Tanya Cabrita, who will almost certainly never read this, but whose concussion treatment helped me resume my studies after an extended break.

Table of Contents

List of Tables

List of Figures

Chapter 1.

Introduction

Capture-recapture (CR) models have been standard tools for studying the dynamics, and assessing the ecological status, of wildlife populations that cannot be counted directly (Chapman, Otis, Burnham, White, & Anderson, 1978; Pledger, Pollock, & Norris, 2010; Royle, Chandler, Sollmann, & Gardner, 2014). In one variant, CR studies are carried out by deploying a set of “detectors” over a desired study area, which record whether animals were present within their vicinity. Detectors can range from traps which physically capture animals, to snares that non-invasively collect an animal’s hair, to acoustic sensors and camera traps (Borchers & Efford, 2008; Royle et al., 2014). Typically, detectors are deployed for multiple sampling sessions, and “detection histories” are created for each detected animal, detailing where and when each animal was both detected and not detected over the course of the study period. These detection histories, along with covariates of interest, are then used as inputs to a CR model.

A wide range of CR models have been created to accommodate various study designs, and animal behaviours. CR models are capable of estimating parameters such as population size and density, survival probabilities, recruitment rates, and animal home range sizes (Borchers & Efford, 2008; Efford & Schofield, 2019; Pradel, 1996; Royle et al., 2014; Schwarz & Arnason, 1996).

This paper focuses on the application of a CR model introduced in Efford & Schofield (2019) to a long-running grizzly bear monitoring project in British Columbia. This model can be classified as an open, and spatially explicit, CR model. It is “open” as it does not assume the population under study is static, instead modelling animals both entering and leaving the population in the study area over time though birth, death, immigration and emigration. It is “spatially explicit” because it directly models the probability of detecting a given animal at a detector as, in part, a function of where it is observed to reside in the study region (Efford & Schofield, 2019; Royle et al., 2014). This model was referred to as OSECR in this paper. OSECR was selected from the open, spatially explicit models available (Gardner, Reppucci, Lucherini, & Royle, 2010; Glennie, Borchers, Murchie, Harmsen, & Foster, 2019; Royle et al., 2014) because it is

relatively fast to fit (especially when compared to Bayesian methods), as well as being fairly well documented and straightforward to implement in the R programming language (R Team Core, 2017).

Since 2006, an ongoing long-term CR study, referred to here as the South Rockies Grizzly Bear Project has been carried out on grizzly bears (*Ursus arctos*) living in a 10 600 km^2 region of the Canadian Rocky Mountains, in south-eastern British Columbia. This region has high abundances of grizzly bear food, and at one point in the late 1980's had the highest recorded grizzly bear density in North America (Lamb, Mowat, McLellan, Nielsen, & Boutin, 2017; McLellan, 1989). This region frequently has undesirable conflicts between bears and humans (Lamb et al., 2017).

Each year, detectors which collect grizzly bear hair were deployed and checked on multiple occasions for hair samples within this study region. Collected hair samples were analyzed using the genetic methods of Paetkau (2003), in an attempt to determine both the sex, and individual identification of the bear which deposited the sample (Lamb, Walsh, & Mowat, 2016). Two different types of detectors have been used over the course of this study: Bait sites (BS), and rub-objects (RO). BS detectors were constructed using the methods of Mowat et al. (2005): Barbed wire was wrapped around groups of trees surrounding a lured bait station containing a non-rewarding lure. When bears came to inspect the lure, they would pass under or over the barbed wire, resulting in hair samples being collected. RO detectors were lengths of barbed wire wrapped around objects frequently rubbed on by bears (typically trees, though power poles or fence posts were also used). When bears rubbed on these objects, the barbed wire would collect hair samples.

Multiple CR analyses have been conducted on South Rockies hair data (Lamb et al., 2017, 2019). In addition, Lamb et al. (2016) used a linear mixed effects model to investigate the average number of grizzly detections per day, broken down by sex, for each detector deployed between 2006 – 2012. Based on Akaike's Information Criterion (Akaike, 1974), these analyses consistently found that detection probability was best modelled as a function of detector type (BS or RO), sex, and season (breeding season or not breeding season), with the detection function usually including a detector type – sex interaction term (Lamb et al., 2016).

An acknowledged shortcoming of these analyses was that multiple studies suggest in addition to sex and detector type, other factors such as bear age, and breeding status can also influence detection probability (Boulanger, Stenhouse, & Munro, 2004; Lamb et al., 2016). For instance, Clapham et al. (2012, 2014) found that all age-sex classes in their study region rubbed on trees, but that the probability of doing so varied by age, sex, and breeding status: Adult males, and adult females with cubs tended to rub more frequently than sub-adults and adult females without cubs. Similarly, Kendall et al. (2009) found that BS detectors could also detect all age-sex classes of bears in their study region, with cubs having lower detection probabilities than other age classes.

While for the South Rockies Grizzly Bear Project, and many other grizzly bear monitoring programs, it is possible to directly include detector type, sex, and season as covariates in the detection probability portion of CR models, age and breeding status cannot be, as this information cannot be easily gathered based on genetic information. For example, in the South Rockies project it is only possible to determine birth year by live-capturing bears. As a result, age data is only available for roughly 10% of all bears detected in this project. As data for these two covariates is rarely collected in large quantities, this prohibits their inclusion in CR analyses, and as result they are often omitted from CR models fit to grizzly bear hair data. Thus, it is possible that many CR parameter estimates, including those in South Rockies Grizzly Bear Project analyses, are biased. This is by no means an uncommon issue, as many ecological processes are highly complex by nature, and can only feasibly be studied using models that likely omit some variables of importance.

In the context of CR models, failing to adequately address heterogeneity in detection probabilities between individual animals results in many of the remaining parameter estimates being noticeably biased (Glennie et al., 2019; Pledger et al., 2010). However, if most variability in detection probability has already been accounted for, the addition of covariates with small effects on detection probability may worsen model performance, as increased variance in parameter estimates could negate the minimal bias reductions. Thus, while the parameter estimates of many models fit to grizzly bear hair data are likely biased, these models may still outperform others with less biased estimates.

This paper's first goal was to quantify how failing to include age in detection function specification affects OSECR estimates of year-to-year survival, per-capita recruitment, home range size, and population growth in South Rockies data. While other parameters, such as population density, can also be estimated via OSECR, only the above were examined. In order to investigate this question, first OSECR models were fit to the full South Rockies Grizzly Bear Project data set and the subset of bears with age data available. The results of these models, as well as the findings of Clapham et al. (2012, 2014) and Kendall et al. (2009), were then used to simulate sets of grizzly bear detection histories where detection probability was a function of sex, detector type (BS or RO), and age. Detection histories were generated over a simulated study region where both BS and RO detectors had been deployed in a similar manner to that of the South Rockies project. Two OSECR models were then fit to these sets of detection histories: one which included the age term that was used when generating the data, and one which did not but was identical to the previous model in all other respects. The distributions of percentage relative bias (PRB) for estimates of each parameter of interest were compared between these two models, as well as each parameter's sample root mean squared error (RMSE). It should be noted that for simplicity's sake, and to reduce computational time, seasonal and breeding-status effects were not included in the simulated detection function, and subsequent analyses.

This study's second goal involved comparing parameter estimates produced using data collected via RO and BS, relative to their typical deployment scheme in the South Rockies Grizzly Bear Project. Specifically, it was of interest whether data from one detector type was more prone to producing biased estimates of parameters of interest when age was unaccounted for in the OSECR detection function. This analysis was carried out by splitting simulated detection histories into two separate sets, where one contained only detection data collected via BS, and the other contained detection data collected via RO. Next, the same two OSECR models described above were fit to these detector-specific detection histories (with any detector type covariates removed), and the PRB distributions of parameters estimates were examined and compared between detector types. Note that only bias was examined in this second analysis, and not RMSE. This is because the current South Rockies sampling scheme, which was similar to the scheme used when simulating capture histories, consists of roughly three times more RO detectors than BS on average (owing mainly to the fact that BS detectors are

much more costly to deploy). Thus, it's likely that parameter estimates derived using RO data would have lower variance than those from BS data by virtue of there being more recorded detections, which could result in lower RMSE. An analysis of which detector type produces overall better estimates (relative to a metric such as RMSE), or what the optimal composition of RO and BS detectors in a study design should be, subject to budget constraints, was not within the scope of this paper.

In the following Methods section, brief overviews of the South Rockies Grizzly Bear Project and the OSECR model are first provided. After this, the simulation studies and subsequent analyses to be performed are outlined.

Chapter 2.

Methods

2.1. South Rockies Grizzly Bear Project Study Design

South Rockies Grizzly Bear Project sampling was carried out using the 'Robust Design' (RD) introduced by Pollock (1982). This sampling scheme divides the study period into a series of "primary" sampling occasions. Population turnover (i.e. births, deaths, immigration, and emigration) is assumed to occur between primary sampling occasions. Within a primary sampling occasion, there are multiple "secondary" sampling occasions where detectors are deployed, and data are collected. It is assumed there is no population turnover between secondary sampling occasions within a primary occasion. Each year of the South Rockies project had a group of consecutive months which were treated as primary sampling occasions, each of which had several secondary occasions within them where data were collected.

Each deployed detector recorded whether a bear was detected on each secondary occasion in the study. The number of detectors deployed over the course of the project fluctuated, as well as the BS:RO ratio: In some years almost only BS detectors were deployed, while others used exclusively RO detectors. In addition, the area over which detectors were deployed changed from year to year, due to changes in landscape and project scope.

For further details on the South Rockies Grizzly Bear Project study design, as well as an exploratory analysis of its data, see Appendix 2.

2.2. The OSECR Model

OSECR detection histories are assumed to come from studies with J primary occasions, each having K_j secondary occasions. An array of S_j detectors are deployed over each primary occasion. Assuming deployed detectors can only record whether an animal was present at a detector during a given secondary occasion, which was the case in the South Rockies project, an individual animal's OSECR detection history, ω_i,

would be a set of J, $K_j \times S_j$ matrices with matrix j having a value of 1 in element (s, k) if animal i was detected at detector s during secondary occasion k of primary occasion j, and 0 if it was not detected then. Note that detectors which collect this type of data are often referred to as 'binary proximity detectors'. The full OSECR detection history, ω, is the collection of these matrices.

There are several ways to parameterize the OSECR model. This analysis will look exclusively at OSECR models which use a half-normal detection function, a Pradel-Link-Barker (PLB) parameterization of apparent survival and recruitment (Efford & Schofield, 2019; Link & Barker, 2005; Pradel, 1996), and treat animal home-range centres as stationary between primary occasions. These conditions are all described below. This class of OSECR model will be referred to as a spatial PLB model.

OSECR assumes detection probabilities between animals are independent, and that multiple detections of the same animal are also independent (after accounting for any necessary covariates). The half-normal model for detection probability has the form:

$$p_{jks} = \lambda_0 \exp\left(-\frac{1}{2\sigma^2}\|\mathbf{X} - t_s\|^2\right),$$

where p_{jks} is the probability of detecting an animal with home-range centre $\mathbf{X}$, over the course of secondary occasion k of primary occasion j, at detector s – located at Cartesian coordinates t_s. An animal's home-range centre can be thought of as the average of all the locations the animal inhabited during the study period. $\|\mathbf{X} - t_s\|$ is the Euclidian distance between the animal's home-range centre and detector s. λ_0 can be thought of as the probability of detecting an animal whose home-range centre precisely coincides with the location of a detector. σ can be thought of as a home-range size parameter, with larger values of σ corresponding to larger home-range sizes. Note that under this detection model, it is assumed that bears have a Gaussian space-usage pattern (Royle et al., 2014). Both λ_0 and σ can be modelled as functions of covariates, often on the logit and log scales respectively.

The PLB parameterization assumes animals only enter the population being studied through birth or permanent immigration, and only exit it through death or permanent emigration. Temporary immigration/emigration is assumed not to occur. Two parameters are used to govern population turnover. The first is apparent survival (ϕ), the probability of an animal not dying/emigrating from the population between two primary

occasions. The second is apparent recruitment (f), the number of animals that were either born or permanently immigrated to the study region between primary occasions i and $i+1$ and remained alive up to primary occasion $i+1$, divided by the number of animals alive at primary occasion i. The terms "apparent survival" and "apparent recruitment" will be used interchangeably with "survival" and "recruitment" in this analysis. These two turnover parameters, along with the half-normal detection function, are used in conjunction to explicitly model each animal's observed detection history. See Efford & Schofield (2019), and Link & Barker (2005) for how this is done. Note that this specific spatial PLB parameterization treats population growth rate, λ, as the derived parameter: $\lambda = \phi + f$. ϕ and f can both be modelled as functions of covariates, typically on the logit and log scales respectively.

While OSECR models can be formulated to model home-range centres as moving between primary occasions (Efford & Schofield, 2019), it was ultimately decided that simulated bear home-range centres in this study would be treated as stationary. As will be seen in later sections, this was primarily decided upon to limit simulation times.

For convenience, this analysis will use the following notation when discussing the spatial PLB models fit: $\phi(*), f(*), \sigma(*), \lambda_0(*)$, where $*$ is a placeholder for the covariates used to model each parameter. Intercept-only models are denoted with a period in place of $*$ (e.g. $f(.)$).

A more extensive overview of OSECR, and related models, can be found in Appendix 1.

2.3. Determining Simulation Study OSECR Parameters

Before detection histories could be simulated, a spatial PLB model needed to be selected to generate detection history data, and reasonable values for this model's parameters needed to be determined.

As 13 years of South Rockies Grizzly Bear Project data were available at the time of this analysis, several spatial PLB models of the form described in Section 2.2 were fit using the *openCR* package (Efford, 2019) in the R programming language to help determine what covariate effects should be included in the model used to generate

simulation study data. Specifically, conditional versions of the above spatial PLB model were fit, which are referred to as '*JSSAsecrfCL'* models in *openCR*. Conditional models condition the OSECR likelihood on the number of animals detected, and tend to be faster to fit than models which use the full likelihood (Efford, 2019). Also note that *openCR* assumes bears are distributed uniformly throughout the study region when fitting OSECR models. This assumption is likely not true for the South Rockies Grizzly Bear Project data and will be further discussed in Section 2.4.

Sex and detector type were both considered as possible parameter covariates when fitting models to South Rockies data. Built-in predictors provided by *openCR*, such as behavioural responses, and primary occasion-specific effects were also explored (Efford, 2019). After fitting several OSECR models to the 2006 – 2018 South Rockies Grizzly Bear Project data set, and comparing them via AIC, it was decided that in simulations, primary occasion-to-primary occasion survival probabilities (ϕ), as well as the home range size parameter (σ), would be modelled as a function of sex, and that per-capita recruitment between primary occasions (f) would be modelled as constant. These relationships were chosen because models that included them tended to be well supported by AIC, they seemed reasonable from a bear biology standpoint, and they were not so complex that they risked greatly slowing down computation time in the simulation study.

The spatial PLB parameter values for survival, recruitment, and home-range size used when simulating detection histories were determined by fitting a $\phi(Sex), f(.), \sigma(Sex), \lambda_0(Sex \times Detector\ Type)$ spatial PLB model with stationary home-range centres to the full South Rockies Grizzly Bear Project data set. See Table 2.1 for these values. While this is likely not the optimal model for this data, its estimates were deemed reasonable to use in the simulation study. λ_0 was parameterized as a two-way interaction between sex and detector type for the derivation of these values because this relationship was often supported by AIC.

Table 2.1. List of OSECR parameters (excluding λ_0) used to generate capture histories for all simulations. These parameters were derived by fitting an OSECR model to 2006 – 2018 South Rockies Grizzly Bear Project data.

ϕ (Males)	ϕ (Females)	f	λ (Males)	λ (Females)	σ (Males)	σ (Females)
0.84	0.89	0.12	0.96	1.01	9970	3634

It was decided that an effect for age in detection probability would be incorporated into simulations through the λ_0 term. λ_0 was selected for this as it would allow for a simple, and biologically intuitive age effect. Specifically, in simulations λ_0 was chosen to be modelled as a three-way interaction on the logit scale between age, sex, and detector type, where age was treated as a factor variable with 3 levels: Yearling (ages 0 to 2), sub-adult (ages 3 to 7), and adult (ages 8 and up). These age classes were selected as they represent three periods in the bear life cycle where behavior and physiology are generally distinct.

Thus, the model used to generate simulated data was a $\phi(Sex), f(.), \sigma(Sex), \lambda_0\ (Sex\ \times Detector\ Type \times Age\ Class)$ spatial PLB model. This model assumes that within sexes, home-range size was independent of age class. It also assumes that the probability of detecting an animal given its home-range centre perfectly overlaps a detector's location was a function of the animal's age class, sex, and the type of detector. It should be restated that this model may not be a completely biologically accurate model for bear behaviour. For instance, there are reasons to assume that both survival and home-range size could also be functions of age class. However, it was believed that this model would still provide a reasonable depiction of bear behaviour, while retaining the parsimony necessary to keep the simulation study's runtime down to an acceptable level.

In order to determine the λ_0 values for each age class-sex-detector type combination for the simulation study, a $\phi(Sex), f(.), \sigma(Sex), \lambda_0(Sex\ \times Detector\ Type \times Age\ Class^*)$ OSECR model was first fit to the subset of detected South Rockies bears with a birth year identified, where $Age\ Class^*$ was a truncated age variable indicating whether a bear was either an adult or not an adult at the time of sampling. This truncated variable was used as the limited data set would not converge when the full age class variable was used. The results of this model, as well subject matter knowledge, and the findings of Clapham et al. (2012, 2014), and Kendall et al. (2009) were then used to derive λ_0 values for the simulation study. Three different sets of λ_0 values were generated for three separate simulation studies: One with small differences in λ_0 values between age classes, one with moderate differences, and one with very large differences. See Table 2.2 for the set of λ_0 values selected. The λ_0 values in Table 2.2 were on the scale of a single day, and thus can be thought of as representing the

probability of detecting a grizzly bear whose home-range centre aligns with the detector location when the detector has been deployed for a single day. As will be further discussed in Section 2.4, simulation studies conducted in this paper assume BS and RO detectors were deployed for multiple days in a row. See Table 2.3 in Section 2.4 for λ_0 values that have been scaled for respective BS and RO deployment lengths using the methods described in Efford, Borchers, & Mowat (2013) for binary proximity detectors.

See Figure 2.1a for plots of the detection functions for each age class of male bears with respect to RO detectors, using λ_0 values from Table 2.2. Note that the detection curves have been scaled assuming the RO detector was deployed for 40 consecutive days, using the methods described in Efford, Borchers, & Mowat (2013) for binary proximity detectors. As can be seen, for a given sex and detector type, detection probabilities between age classes are proportional to each other. In addition, see Figure 2.1b for plots of the total area each sex of bear was assumed to spend 95% of its time under the half-normal detection function, using the σ values from the simulation procedure.

The sets of λ_0 values used in the first two simulation studies were selected to take on values which could plausibly occur in nature. The λ_0 values in the third simulation study were selected mainly to produced very large discrepancies in detection probabilities between age classes within a given sex and detector type, which were unlikely to occur in this field of study. This was done to test the robustness of parameter estimates when a very large age effect had been omitted from the model.

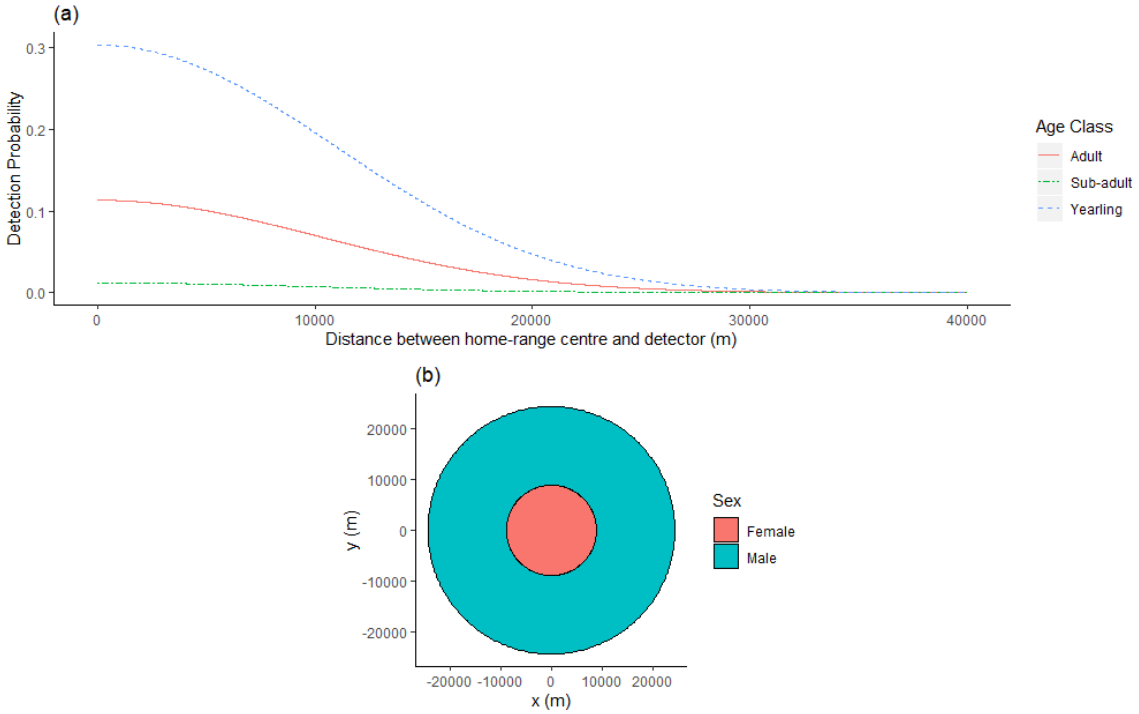

Figure 2.1. **a) Detection probability curves for males of each age class at a RO detector that has been deployed for 40 days. λ_0 values were taken from scenario 2: λ_0 – Moderate. b) Regions where bears are assumed to spend 95% of their time under a half-normal detection function, using the σ values from Table 2.1.**

Table 2.2. List of λ_0 values used in the 3 different simulated scenarios examined in this study (small difference in $\lambda_0$values between age classes, moderate difference in λ_0 values, and a large difference in λ_0 values). Note that λ_0 values have been scaled to represent the probability of detecting an animal whose home-range centre coincides with the location of a detector when the detector has been deployed for only a single day. Detection probabilities when detectors have been left for multiple days can be calculated using the methods described in (Efford et al., 2013).

Sex	Age Class	Detector Type	λ_0 - Small	λ_0 - Moderate	λ_0 - Large
F	Adult	BS	0.015	0.01	0.01
F	Sub-adult	BS	0.035	0.07	0.15
F	Yearling	BS	0.001	0.0005	0.0005
F	Adult	RO	0.0015	0.0001	0.0001
F	Sub-adult	RO	0.003	0.003	0.02
F	Yearling	RO	0.005	0.009	0
M	Adult	BS	0.004	0.015	0.1
M	Sub-adult	BS	0.002	0.005	0.01
M	Yearling	BS	0.001	0.0005	0.0005
M	Adult	RO	0.0008	0.003	0.02
M	Sub-adult	RO	0.0006	0.0003	0.01
M	Yearling	RO	0.005	0.009	0

2.4. Simulation Study Design

100 sets of detection histories were simulated for each set of λ_0 values. Data was simulated over a 150 km x 150 km study region. Bear home-range centres could be located anywhere within the region, while detectors were placed within a 50 km x 50 km square located at the centre of the region. In order to match the detector placement scheme of the South Rockies Grizzly Bear Project, BS detectors were placed in a uniform grid with 14 km spacing, while RO detectors were randomly distributed throughout the detector region with the constraint that there must be a minimum distance of 500 m between any two detectors. BS locations were consistent across all simulated data sets, while RO locations varied. A 3:1 ratio between the number of RO and BS detectors was used, resulting in 16 BS, and 48 RO detectors being deployed in each simulated data set.

In each simulated capture history, sampling took place over five equally spaced primary sampling occasions (years), each of which having four secondary occasions.

RO detectors were deployed for 40 days in each secondary occasion, while BS detectors were deployed for 14 days in the first two secondary occasions of every primary occasion, and we not deployed in the last two. These time periods were chosen to roughly match the sampling intervals in the South Rockies project.

RO detectors are left out longer each secondary sampling secondary occasion and are also deployed for more secondary occasions than BS detectors. As such, Table 2.2 does not paint a clear picture of the differences in detection probabilities between the two detector types. To aid with this, see Table 2.3, which contains the probability of detecting a grizzly bear whose home-range centre is precisely at the location of a detector, over the course of a secondary occasion, for each age class-sex-detector type combination in the simulation study. This probability was calculated using the equation $p = 1 - (1 - \lambda_{0-C})^{T_D}$, where p is detection probability, λ_{0-C} is the λ_0 value found in Table 2.2 for a given age class-sex-detector type combination, and T_D is the number of days during which the given detector type was deployed (Efford et al., 2013).

Table 2.3. Probabilities of detecting bears from each age-sex class over the course of a simulated secondary occasion – 14 days for a BS detector, and 40 days for a RO detector – when their home-range centres overlap a detector. These λ_0 were calculated by rescaling the λ_0 in Table 2.2 using the methods for binary proximity detectors found in Efford et al. (2013).

Sex	Age	Detector Type	λ_0- Small	λ_0- Moderate	λ_0- Large
F	Adult	BS	0.19	0.13	0.13
F	Sub-adult	BS	0.39	0.64	0.90
F	Yearling	BS	0.014	0.0070	0.0070
F	Adult	RO	0.058	0.0040	0.0040
F	Sub-adult	RO	0.11	0.11	0.55
F	Yearling	RO	0.18	0.30	0
M	Adult	BS	0.055	0.19	0.77
M	Sub-adult	BS	0.028	0.068	0.13
M	Yearling	BS	0.014	0.0070	0.0070
M	Adult	RO	0.032	0.11	0.55
M	Sub-adult	RO	0.024	0.012	0.33
M	Yearling	RO	0.18	0.30	0

Bear home-range centre locations were assumed to be the result of an inhomogenous Poisson process. The specific home-range centre density function used in simulations was constructed to resemble the estimated distribution of bears found in

the CR analysis of South Rockies data conducted in Lamb et al. (2019). A heat map of this simulated distribution can be found in Figure 2.2. Home-range centres were sampled from this distribution using Accept-Reject sampling (Robert, 2004). The initial population size in each round of simulations was treated as a Poisson random variable with mean equal to the integral of the density function ($Pois(\lambda = 285.77)$). See Figure 2.3 for a plot of a simulated detector layout, along with home-range centres drawn from this distribution.

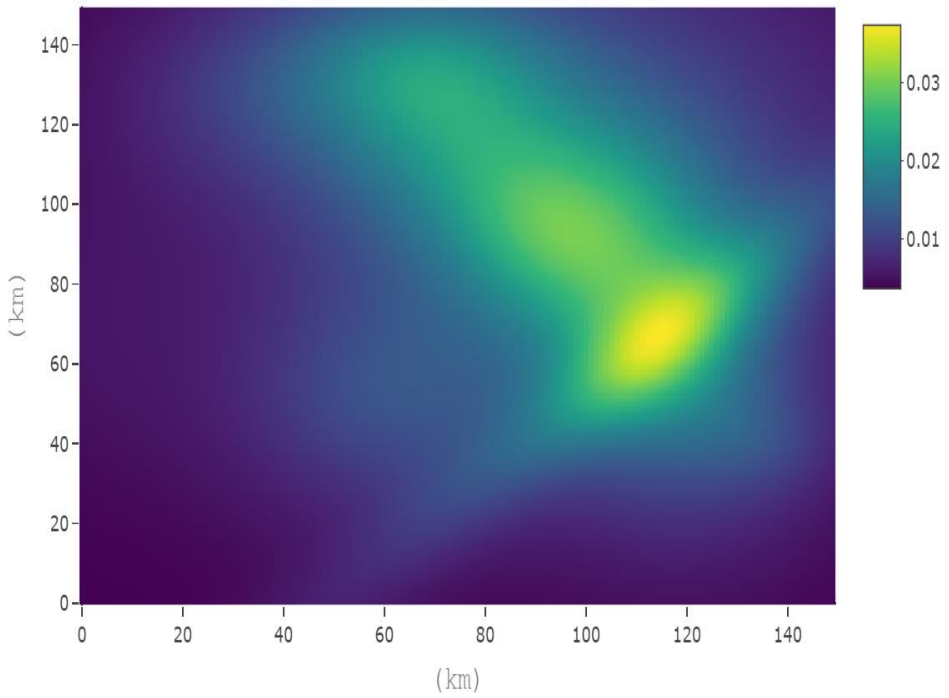

Figure 2.2. Heatmap of the inhomogeneous density function that home-range centres in each simulation are drawn from using Accept-Reject sampling. The simulated study region is 150km x 150 km.

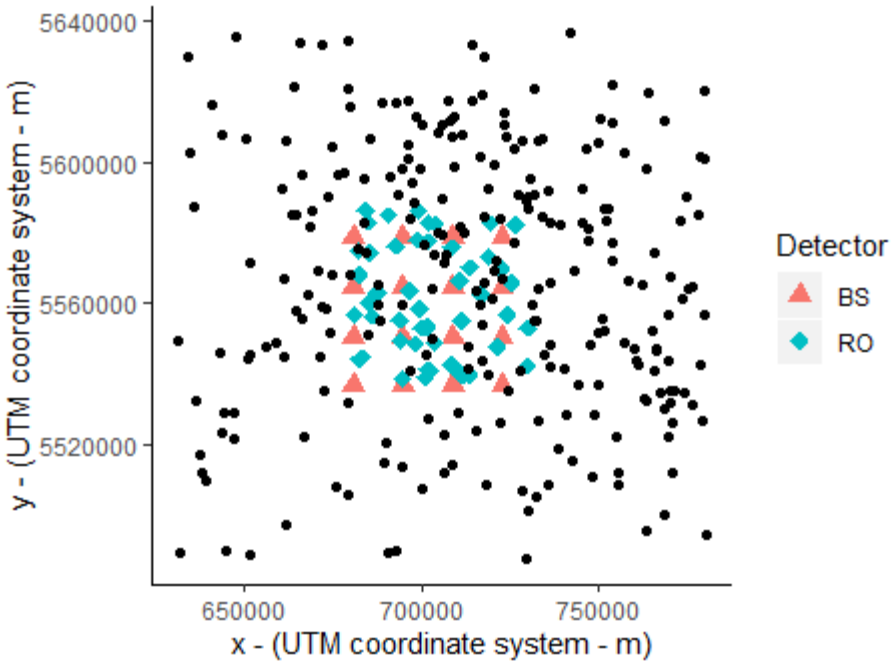

Figure 2.3. An example of the detector layout, and initial distribution bear home-range centres (black) used in a round of simulations. The detector layout was the same over the 5 simulated years, while the distribution of home-range centres changed as bears entered and exited the population.

openCR assumes bear home-range centres are distributed uniformly over the study region. This assumption will be violated as home-range centre density function was non-uniform. However, the effects of this violation were likely negligible, as draws from the simulation study's home-range centre distribution typically looked similar those from a uniform distribution, for the population sizes under consideration in this study. See Figure 2.3 for an example of this; note how home-range centres appear as if they could have been drawn from a two-dimensional uniform distribution.

The number of bears in each age-sex class was treated as a multinomial variable, with probabilities equal to the estimated average age-sex proportions in the study region (Table 2.4).

Table 2.4. Proportions used to generate the number of bears of each age-sex class in simulated capture histories. Initial age-sex class counts are treated as a draw from a Multinomial distribution, using the proportions in this table as parameter values.

Prop. Yearling Male	Prop. Sub-adult Male	Prop. Adult Male	Prop. Yearling Female	Prop. Sub-adult Female	Prop. Adult Female
0.11	0.18	0.12	0.11	0.2	0.28

After generating the initial population, detections histories for each bear were created for the first primary occasion. Next, the number of bears lost through apparent death (i.e. death and permanent emigration from the study region) and gained through apparent recruitment (i.e. birth or permanent immigration into the study region) were calculated. This was repeated for the remaining 4 primary sampling occasions. The number of male and female apparent deaths ($Deaths + Permanent\ Emigration$) were each treated as binomial random variables, with the sex-specific death rates ($1 - \phi_{Females/Males}$) as "success" probabilities. Similarly, the number of apparent births ($Births + Permanent\ Immigration$) were also treated as a binomial random variable, with the per-capita recruitment rate as the success probability. (Note that in practice per-capita recruitment can be greater than 1, and thus apparent births should normally not be modelled as binomial; however, in this simulation study's case the selected per-capita recruitment rate was well below 1, and the resulting binomial variable had nearly equivalent variance to an analogous Poisson random variable.) All new entrants to the population were assigned an age-sex class using the Multinomial method described earlier.

In addition, it was assumed that bears did not age over years, and retained their starting age-sex class for the duration of the simulation study. This choice was made so that population demographics stayed relatively constant around their average values for each simulation. This is a simplifying assumption as the age-sex composition of grizzly bear populations can often fluctuate noticeably from year-to-year and is a function of several factors.

Once all simulated detection histories had been generated, the histories from each round of simulations had a $\phi(Sex), f(.), \sigma(Sex), \lambda_0(Sex * Detector\ Type * Age\ Class)$ spatial PLB model fit to them, referred to here as the correct model (M_c), as well as a $\phi(Sex), f(.), \sigma(Sex), \lambda_0(Sex * Detector\ Type)$ spatial PLB model fit to them –

the closest to the true model that can be fit with the data available in the South Rockies Grizzly Bear Project, hence referred to as the biased model (M_b). The distribution of the observed PRB for estimates of ϕ_{Males}, $\phi_{Females}$, f, $\lambda_{Males}(= \phi_{Males} + f)$, $\lambda_{Females}(= \phi_{Females} + f)$, σ_{Males}, and $\sigma_{Females}$ were plotted and compared between M_c and M_b. In addition, RMSE were calculated for each of these parameters and compared between models. Both M_c and M_b correctly assume home-range centres are stationary.

These same models (minus the detector type covariate) were then refit on RO and BS detection data separately, with the same parameter estimates' PRB distributions analyzed, and compared between detector types. This was carried out to investigate how prone the two detector types were, relative to their deployment methodologies in the South Rockies Grizzly Bear Project, to producing biased parameter estimates.

A total of 1800 spatial PLB models were fit in this simulation study (600 for each set of λ_0 values). All models were fit using *openCR*'s default maximization procedure. *openCR* discretizes the study region into a series of points that serve as possible home-range centres for detected animals, which are associated with pixels of equal area, resulting in several integrals in the OSECR likelihood being replaced by summations (Efford & Schofield, 2019). This analysis modeled the study region as a grid with 3 km spacing between points, that extended 40 km outwards from the perimeter of the detector array. This 40 km distance is often referred to as a 'buffer' width, and was selected as all the detection functions used in simulations essentially reach a value of 0 40 km away from a given detector.

Chapter 3.

Results

Results of the three simulation studies are presented in this section. Each sub-section contains boxplots comparing the distribution of PRB for each parameter of interest between M_c and M_b, for the full simulated detection data set, the BS only data set, and the RO only data set. The standard boxplot layout was used, with box edges representing the data's first and third quartiles, and the line inside each box marking the data's median. Whiskers extend 1.5 times the inter-quartile range from the median. In addition, sample mean PRB are marked as points on each box for every parameter of interest, along with corresponding unadjusted 95% Wald confidence intervals. Parameters were classified as having potentially biased estimates by examining their distribution and observing whether the confidence intervals for mean PRB contained 0. As these intervals are unadjusted, they were used more to help identify parameters whose estimates may be biased enough that they potentially limit the utility of M_b, than to conclusively test that there was some level of bias present. Intervals adjusted for multiple comparisons were not included as a very large number of comparisons would have to be made for each simulation study, which would likely cause confidence intervals to be overly conservative.

Boxplots were arranged so that M_c and M_b could be easily compared, and can be found in subsections 3.1 – 3.3. Each subsection also includes tables listing and comparing RMSE of parameters of interest from the two models, as well as summary of the results for each simulated scenario. See Section 4.1 for an interpretation of simulation results in the context of the South Rockies Grizzly Bear Project. See Appendix 3.1 for boxplots arranged for easy comparison of PRB distributions between detector types, within the same simulated scenario. Also see Appendix 3.2 for tables containing summary statistics of PBR for each model fit in the three simulated scenarios.

The results of four models were removed from Figure 3.2 because they contained very large $\hat{\sigma}_{Males}$ outlier values, caused by model convergence issues. The parameter estimates for these models can be found in Appendix 3.2.

There were several instances during all three scenarios in the simulation study where *openCR*'s default maximization algorithm issued warnings about possible convergence errors. The results from these models were included in analyses anyway (except for the four extreme outliers mentioned above). While *openCR* does accommodate more robust optimization routines, these generally take longer to converge than the default algorithm, and overall run-time was already a major concern for this study. In addition, the full South Rockies Grizzly Bear Project data set is considerably larger than the simulated capture histories in this study, with models fit using the fast default maximization algorithm already taking on the scale of days to weeks to fit in some cases. Thus, it will not always be practical to use even slower algorithms in conjunction with the *openCR* package, and so it was of interest to examine how reliable *openCR* estimates were even when convergence criteria were not necessarily met.

3.1. $\lambda_0 - Small$

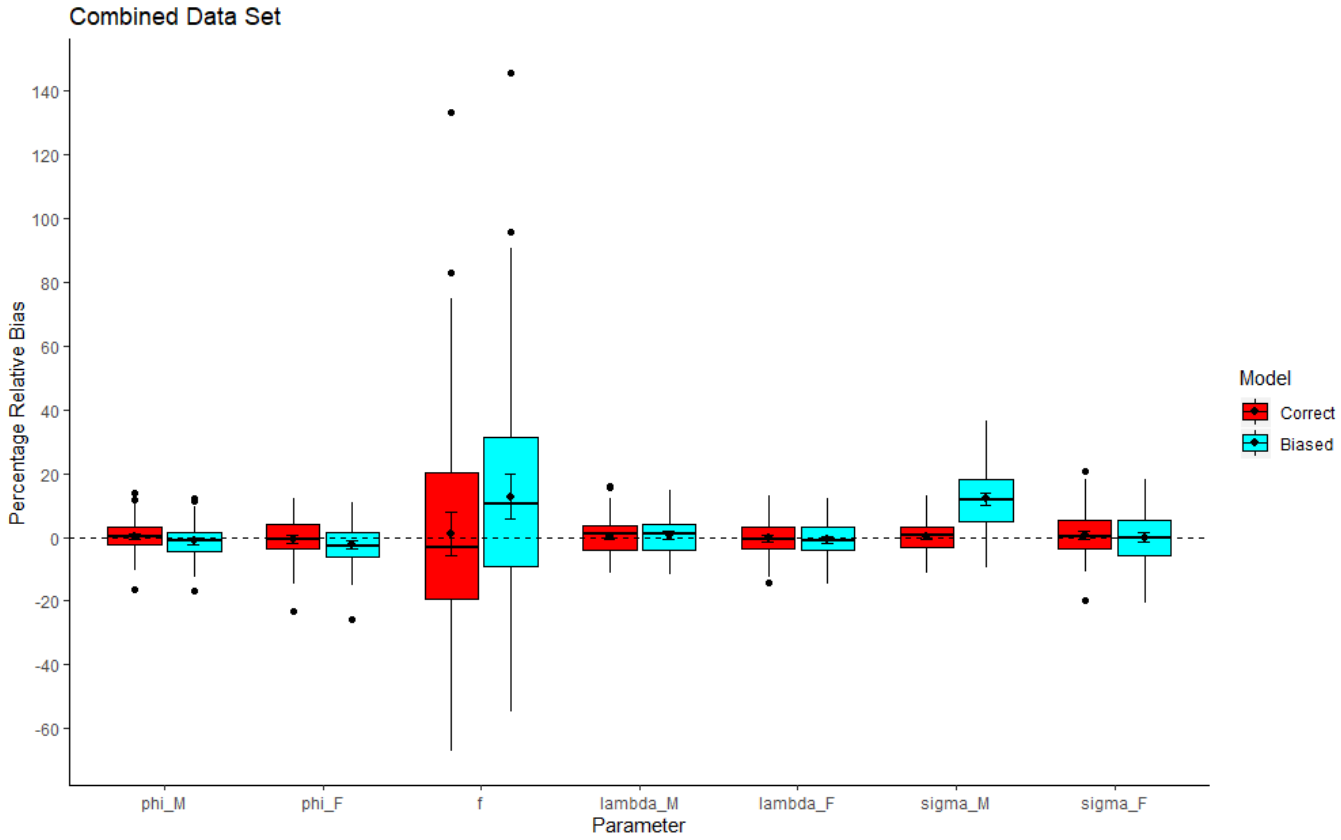

Figure 3.1. **Standard boxplots of percentage relative bias (PRB) for each parameter of interest in M_c and M_b, using detections from both BS and RO detectors, for the λ_0 – Small simulated scenario. Whiskers extend a distance of 1.5 time the inter-quartile range from the median. Sample mean PRB along with corresponding 95% confidence intervals are also included. The results from 100 rounds of simulations were included in this figure.**

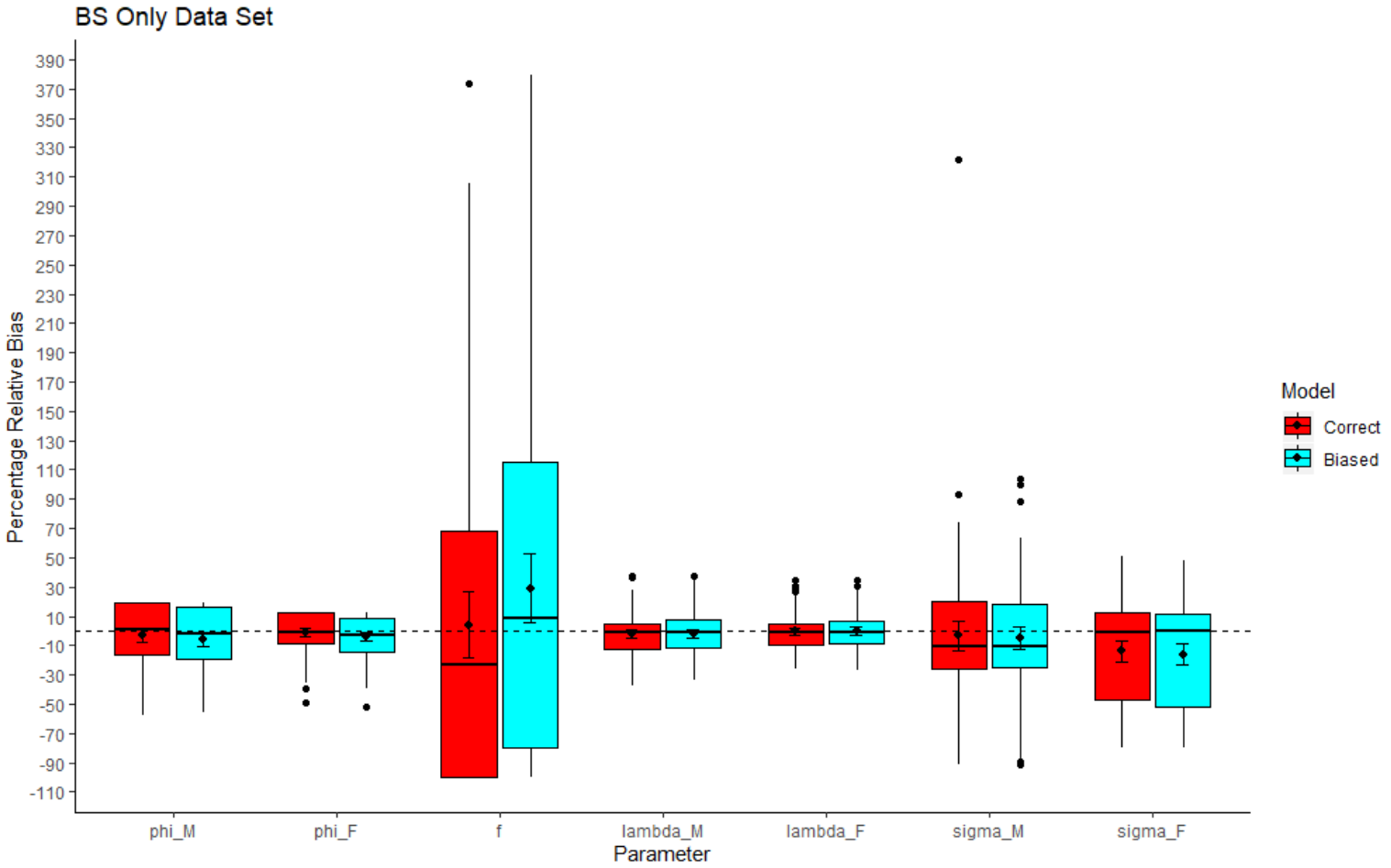

Figure 3.2. **Standard boxplots of percentage relative bias (PRB) for each parameter of interest in M_c and M_b, using only detections at BS detectors, for the λ_0 – Small simulated scenario. Whiskers extend a distance of 1.5 time the inter-quartile range from the median. Sample mean PRB along with corresponding 95% confidence intervals are also included. The results from 96 rounds of simulations were included in this figure (the results from four rounds were removed due to very large outliers).**

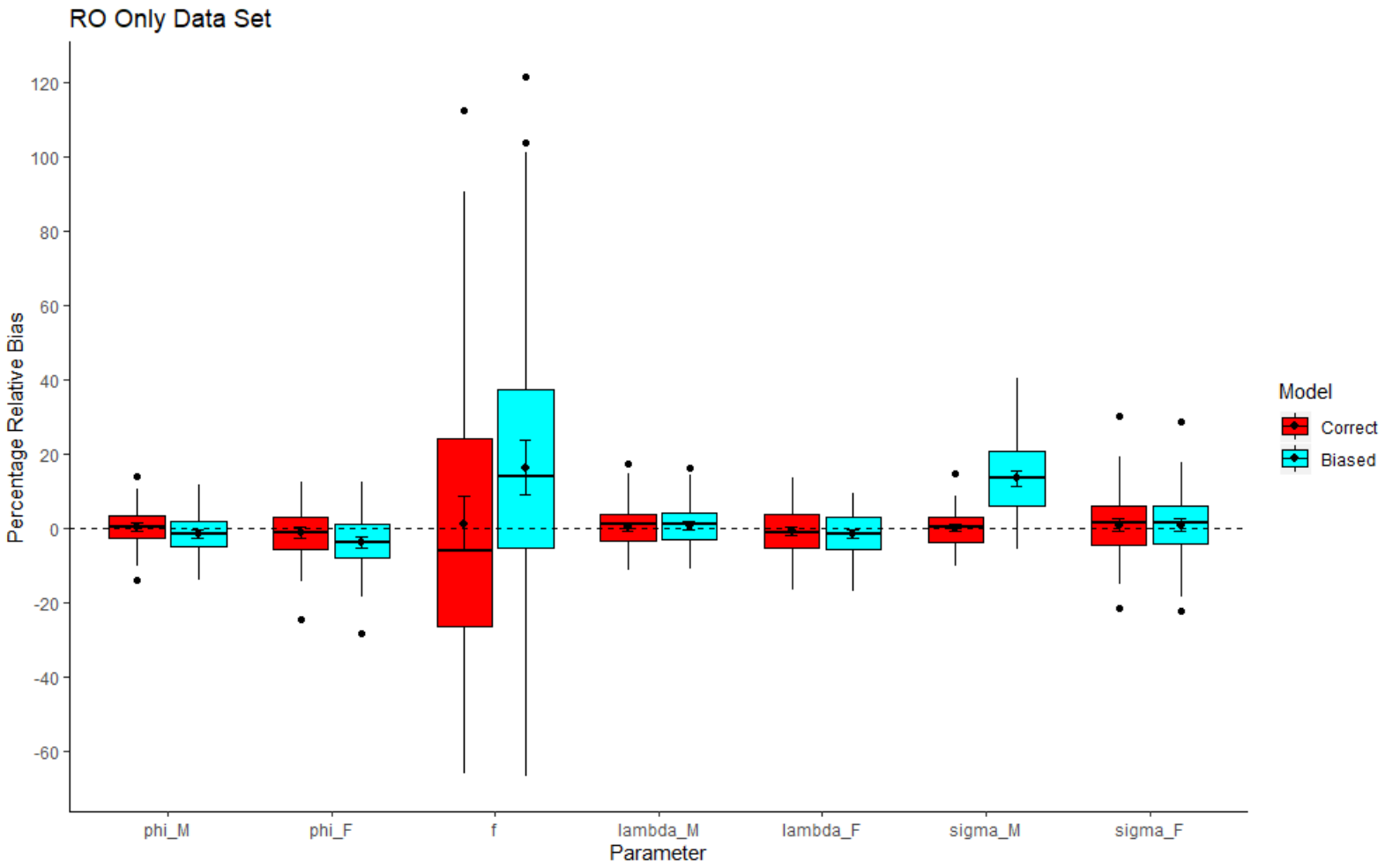

Figure 3.3. **Standard boxplots of percentage relative bias (PRB) for each parameter of interest in M_c and M_b, using only detections at RO detectors, for the λ_0 – Small simulated scenario. Whiskers extend a distance of 1.5 time the inter-quartile range from the median. Sample mean PRB along with corresponding 95% confidence intervals are also included. The results from 100 rounds of simulation were included in this figure.**

Table 3.1. Sample root mean squared error (RMSE) values for each parameter of interest in M_c and M_b, along with their ratio, for the λ_0 – Small simulated scenario using the full simulated data.

Parameter	Simulation Value	RMSE (M_c)	RMSE (M_b)	RMSE (M_b)/RMSE (M_c)
f	0.12	0.0406	0.044	1.08
$\lambda_{Females}$	1.01	0.0551	0.053	0.96
λ_{Males}	0.96	0.0528	0.052	0.99
$\phi_{Females}$	0.89	0.0574	0.060	1.04
ϕ_{Males}	0.84	0.0434	0.046	1.06
$\sigma_{Females}$	3634	253.1808	270.470	1.07
σ_{Males}	9970	446.3984	1500.337	3.36

Figure 3.1 shows that with respect to the full data set, there appeared to be noticeable biases introduced in M_b. $\hat{\phi}_{Females}$ and $\hat{\phi}_{Males}$ were biased downwards (Mean PRB $= -2.5\%$ and -1.1% respectively), while $\hat{f}$ and $\hat{\sigma}_{Males}$ were biased upwards (Mean PRB $= 12.8\%$ and 12.0% respectively). Based on the scales of $\phi_{Females}$, ϕ_{Males}, and f, these observed biases are not too large: A -2.5% PRB in $\hat{\phi}_{Females}(= 0.89)$ corresponds to a biased $\phi_{Females}$ estimate (denoted here as $\tilde{\phi}_{Females}$) of $\tilde{\phi}_{Females} = 0.86775$, a -1.08% PRB in $\hat{\phi}_{Males}(= 0.84)$ corresponds to $\tilde{\phi}_{Males} = 0.830928$, and a 12.8% PRB in $\hat{f}$ $(= 0.12)$ corresponds to $\tilde{f} = 0.13536$. (Note that a portion of the positive bias in $\hat{f}$ could be a function of its chosen value being close to 0: There were instances where $PRB(\hat{f}) > 100\%$, however downward bias was limited to $PRB(\hat{f}) = -100\%$). The bias in σ_{Males} estimates is more substantial however. A 12.0% PRB in $\hat{\sigma}_{Males}(= 9970)$ corresponds to $\tilde{\sigma}_{Males} = 11166.4$. For context, under the half-normal detection function this corresponds to the predicted area in which bears spend 95% of their time being roughly 25% larger than it actually is. These same patterns were also observed in the RO only data set, with the exception of a small negative bias (PRB $= -1.41\%$) being observed for $\lambda_{Females}$ estimates (see Figure 3.3).

Moving to the BS only analysis, Figure 3.2 indicated that in addition to bias likely being present in M_b parameters, M_c may also biased for $\hat{\sigma}_{Females}$. The distribution of M_c estimates of f and σ_{Males} and $\sigma_{Females}$ also appeared skewed, which is less favourable than estimates being clustered around their true value. The likely reason these patterns in M_c estimates were present for the BS data and not the RO data set is that while BS in this scenario tended to have higher age-sex class detection probabilities than RO

overall, this was not enough to compensate for the fact that there were 3 times more RO deployed, for twice as many secondary occasions. Likely, a combination of not getting enough recaptures to properly estimate home-range shapes and sizes, combined with possible convergence issues caused by a small data set, led to the bias and skewed distributions observed in M_c. This is supported by the fact that the bias and skew in σ_{Males} and $\sigma_{Females}$ estimates were reduced in M_c models fit to BS only data in the λ_0 – Moderate simulated scenario (see Figure 3.5), which had higher average detection probabilities for both male and female bears (M_c still appeared biased for $\hat{f}$ however, which is discussed in Section 4.2).

In the full data set, Figure 3.1 does not seem to imply there was any noticeable decrease in parameter variability under M_b compared to M_c. In fact, in some cases, such as for σ_{Males}, estimates seem more variable under M_b. In addition, Table 3.1 shows that in general, M_c outperformed M_b in terms of RMSE. The only exceptions were for λ_{Males} and $\lambda_{Females}$, which had lower RMSE under M_b. Thus, it appears that overall M_c outperformed M_b. Although using M_b instead of M_c will often yield fairly reliable estimates of most parameters (as the PRB observed relative to the size of many of the parameters was not very large), with σ_{Males} being the main exception.

3.2. $\lambda_0 - Moderate$

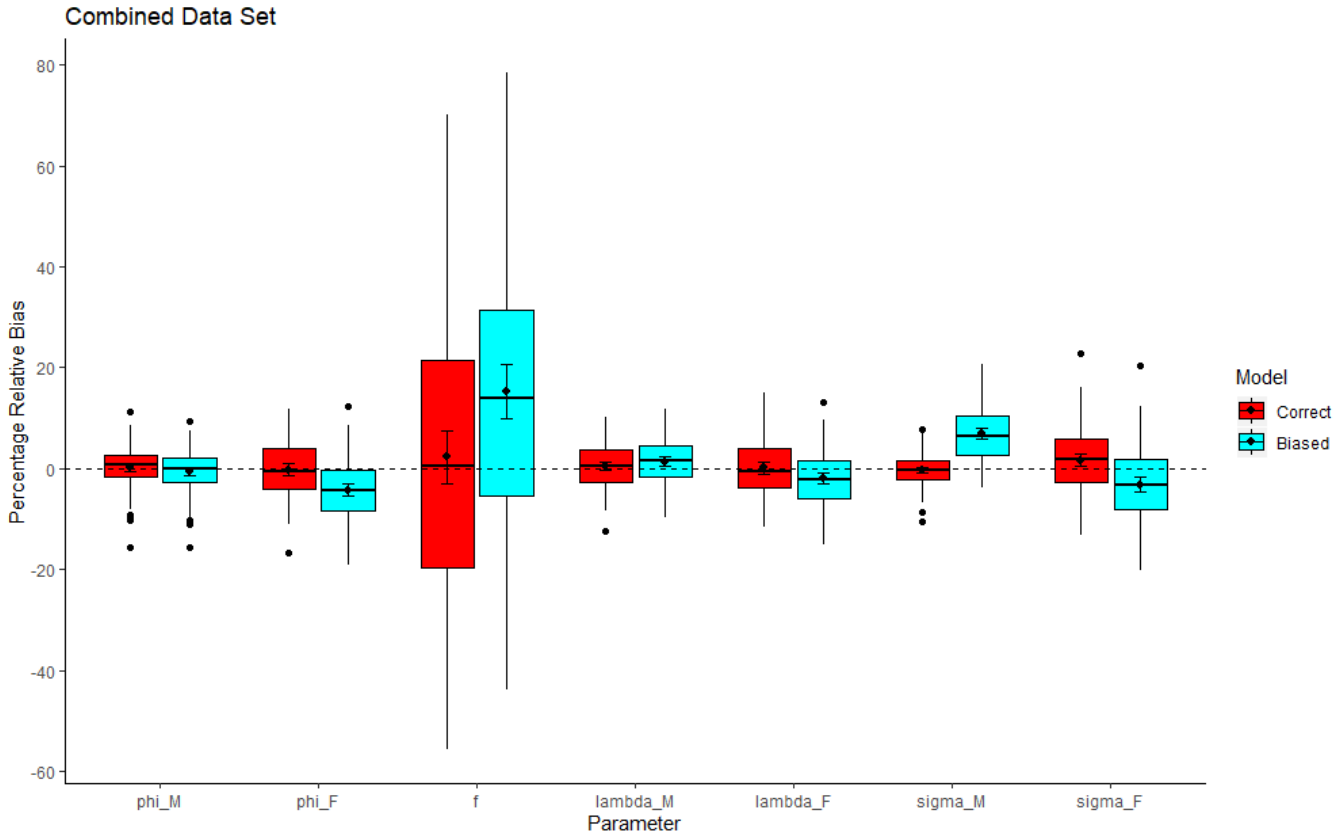

Figure 3.4. **Standard boxplots of percentage relative bias (PRB) for each parameter of interest in M_c and M_b, using detections from both BS and RO detectors, for the λ_0 – Moderate simulated scenario. Whiskers extend a distance of 1.5 time the inter-quartile range from the median. Sample mean PRB along with corresponding 95% confidence intervals are also included. The results from 100 rounds of simulation were included in this figure.**

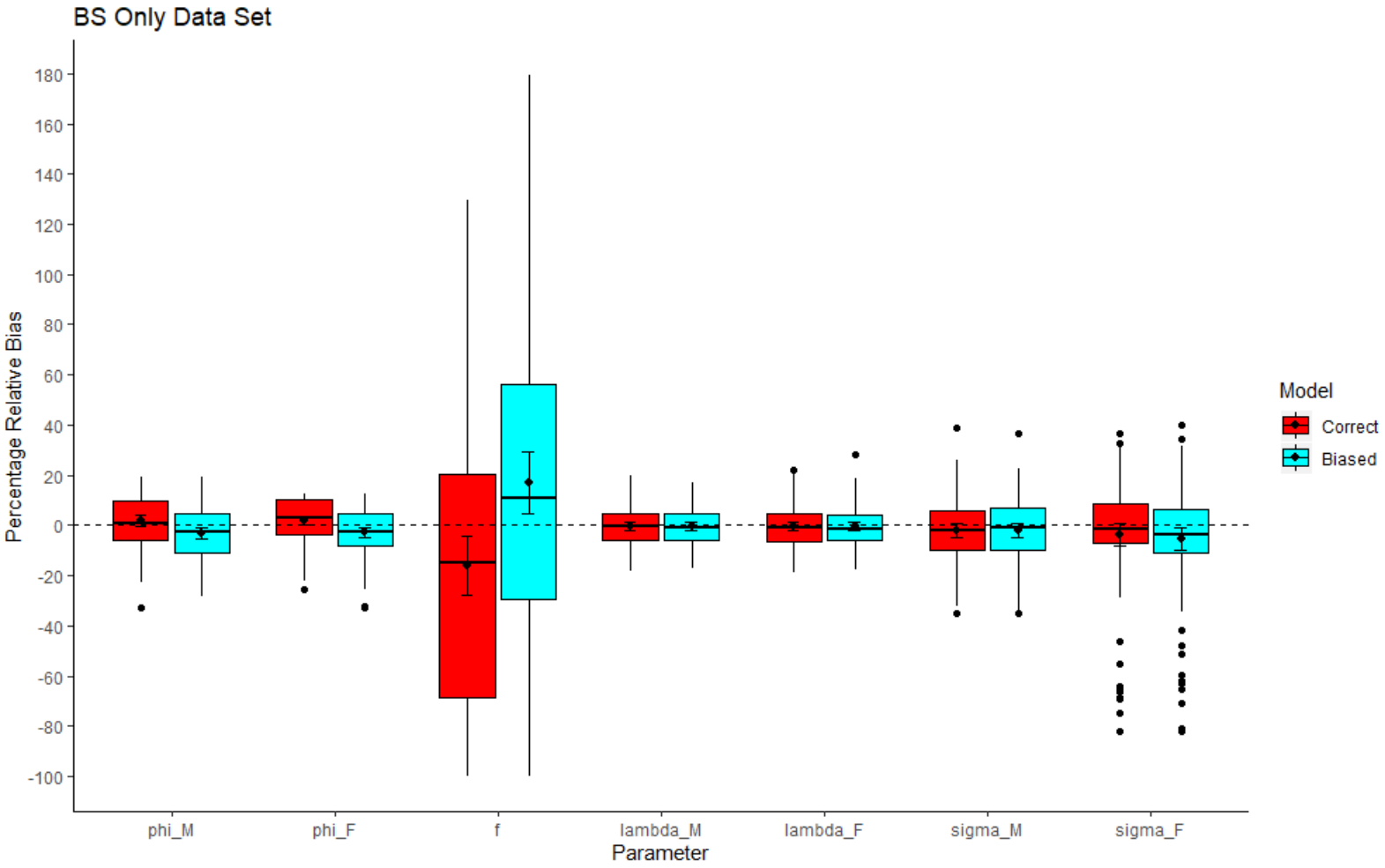

Figure 3.5. **Standard boxplots of percentage relative bias (PRB) for each parameter of interest in M_c and M_b, using only detections at BS detectors, for the λ_0 – Moderate simulated scenario. Whiskers extend a distance of 1.5 time the inter-quartile range from the median. Sample mean PRB along with corresponding 95% confidence intervals are also included. The results from 100 rounds of simulation were included in this figure.**

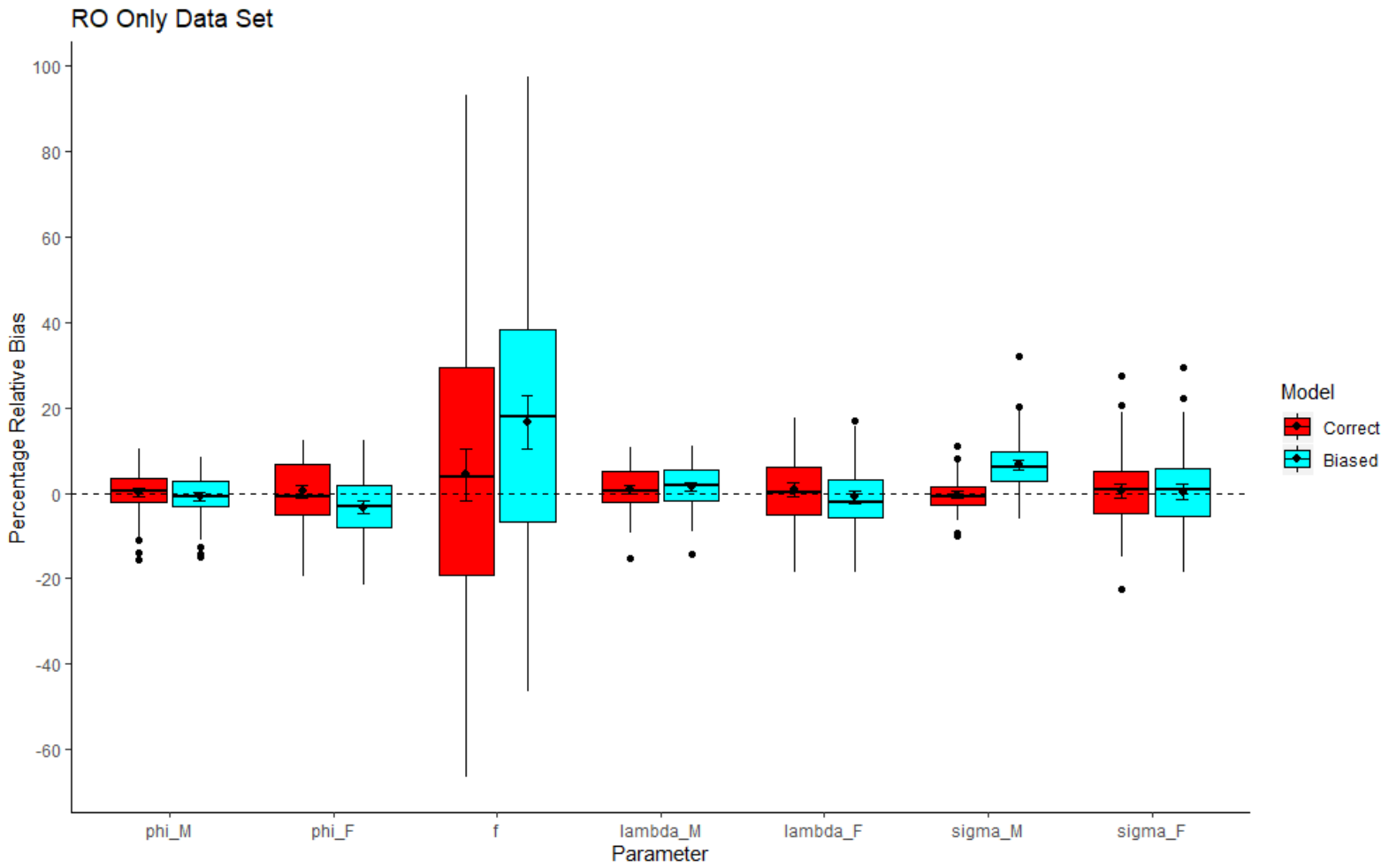

Figure 3.6. **Standard boxplots of percentage relative bias (PRB) for each parameter of interest in M_c and M_b, using only detections at RO detectors, for the λ_0 – Moderate simulated scenario. Whiskers extend a distance of 1.5 time the inter-quartile range from the median. Sample mean PRB along with corresponding 95% confidence intervals are also included. The results from 100 rounds of simulation were included in this figure.**

Table 3.2. Sample root mean squared error (RMSE) values for each parameter of interest in M_c and M_b, along with their ratio, for the λ_0 – Moderate simulated scenario using the full simulated data.

Parameter	Simulation Value	RMSE (M_c)	RMSE (M_b)	RMSE (M_b)/RMSE (M_c)
f	0.12	0.0322	0.0376	1.167
$\lambda_{Females}$	1.01	0.0570	0.0594	1.042
λ_{Males}	0.96	0.0430	0.0441	1.025
$\phi_{Females}$	0.89	0.0520	0.0643	1.235
ϕ_{Males}	0.84	0.0370	0.0378	1.020
$\sigma_{Females}$	3634	250.016	295.020	1.180
σ_{Males}	9970	334.838	888.201	2.653

Figure 3.4 shows that, like the first simulation study, there was bias introduced by M_b when fitting models to the full data set. This was most noticeable for $\hat{\phi}_{Females}$ (Mean PRB $= -4.2\%$), $\hat{f}$ (Mean PRB $= 15.4\%$), $\hat{\sigma}_{Males}$ (Mean PRB $= 6.9\%$), and $\hat{\sigma}_{Females}$ (Mean PRB $= -3.2\%$). Comparing Tables A3.1 and A3.4, it appears that M_b bias tended to be higher in the second simulated scenario (with $PRB(\hat{\sigma}_{Males})$ being the biggest exception), which is not surprising given a larger effect had been omitted in it. In addition, compared to the other parameters in M_c, and relative to the size of the parameter, the Mean PRB of $\hat{\sigma}_{Females}$ ($= 1.7\%$) is somewhat high. The unadjusted 95% confidence interval for mean PRB of $\hat{\sigma}_{Females}$ also narrowly excludes 0. There is no clear reason why this parameter should be biased upwards, other than this being an artifact of too few simulations or having been caused by convergence issues.

Like in the first simulation study, the pattern of biases in the RO only analysis was similar to the full data set's (see Figure 3.6), with the main exception being that it lacked the M_b $\hat{\sigma}_{Females}$ bias observed in the full data set. However, the bias pattern in the BS only analysis (see Figure 3.5) was different from the other two analyses. Specifically, the BS only analysis results did not contain the $\hat{\sigma}_{Males}$ M_b bias observed in the other two. This difference is likely a function of the structure of the omitted age class effect, and potentially the difference in layouts of the two classes of detectors. M_c estimates of f in the BS only analysis appeared biased overall. This was likely caused by some combination of convergence issues, f being a small quantity, or the results being an artifact of too few simulations.

As in the λ_0 – Small scenario, there does not appear to be a large difference in the variability of parameters estimates between M_c and M_b when using the full simulated data set (see Figure 3.4). Thus, it is not surprising that RMSE values were higher for all parameters in M_b. Once again, the differences in RMSE varied from small (e.g. ϕ_{Males}), to quite large (e.g. σ_{Males}). It should be noted that once again, except for the home-range parameters, the PRB introduced in M_b are not very large when the scale of the parameters being estimated is considered.

3.3. $\lambda_0 - Large$

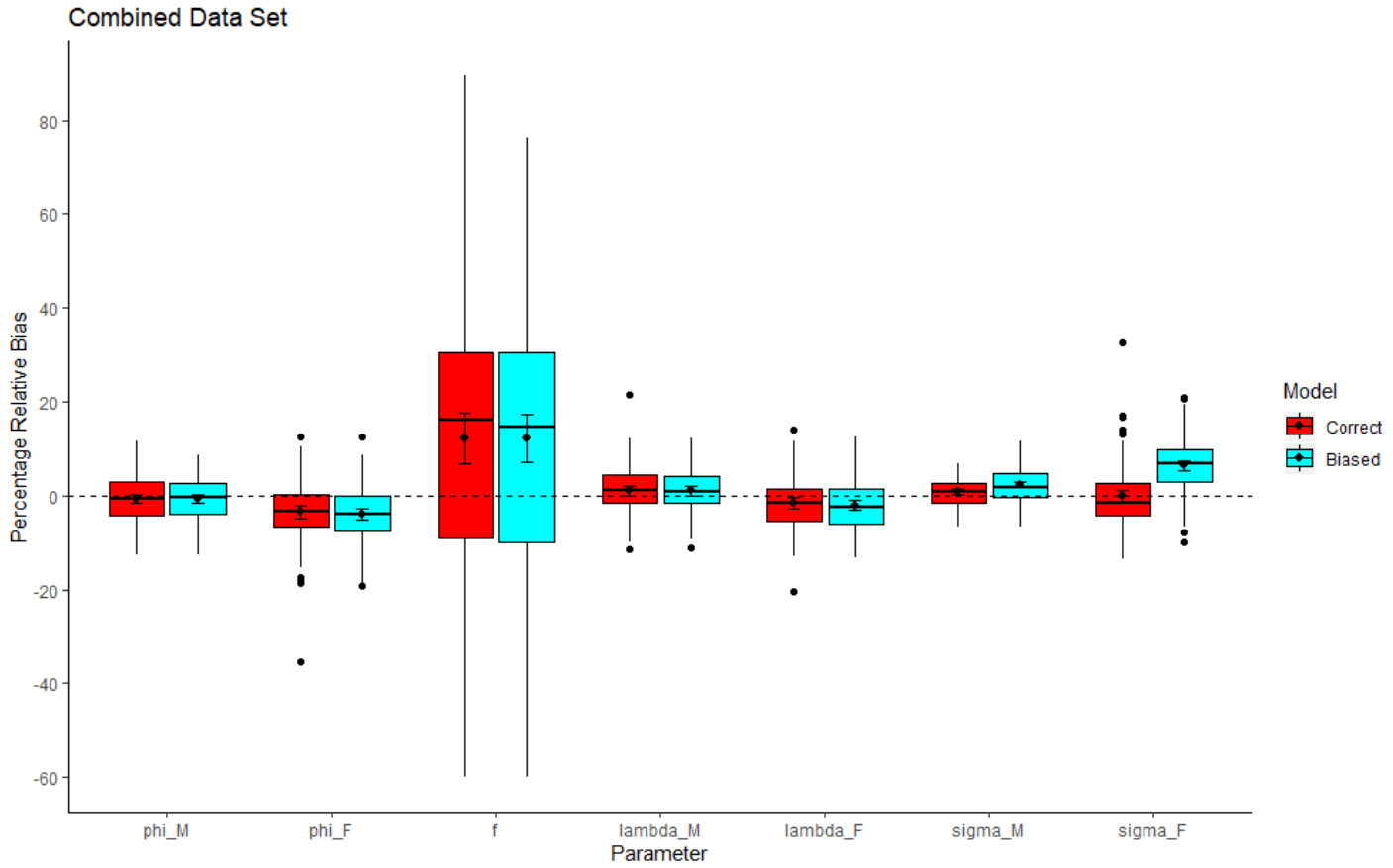

Figure 3.7. **Standard boxplots of percentage relative bias (PRB) for each parameter of interest in M_c and M_b, using detections from both BS and RO detectors, for the λ_0 – Large simulated scenario. Whiskers extend a distance of 1.5 time the inter-quartile range from the median. Sample mean PRB along with corresponding 95% confidence intervals are also included. The results from 100 rounds of simulation were included in this figure.**

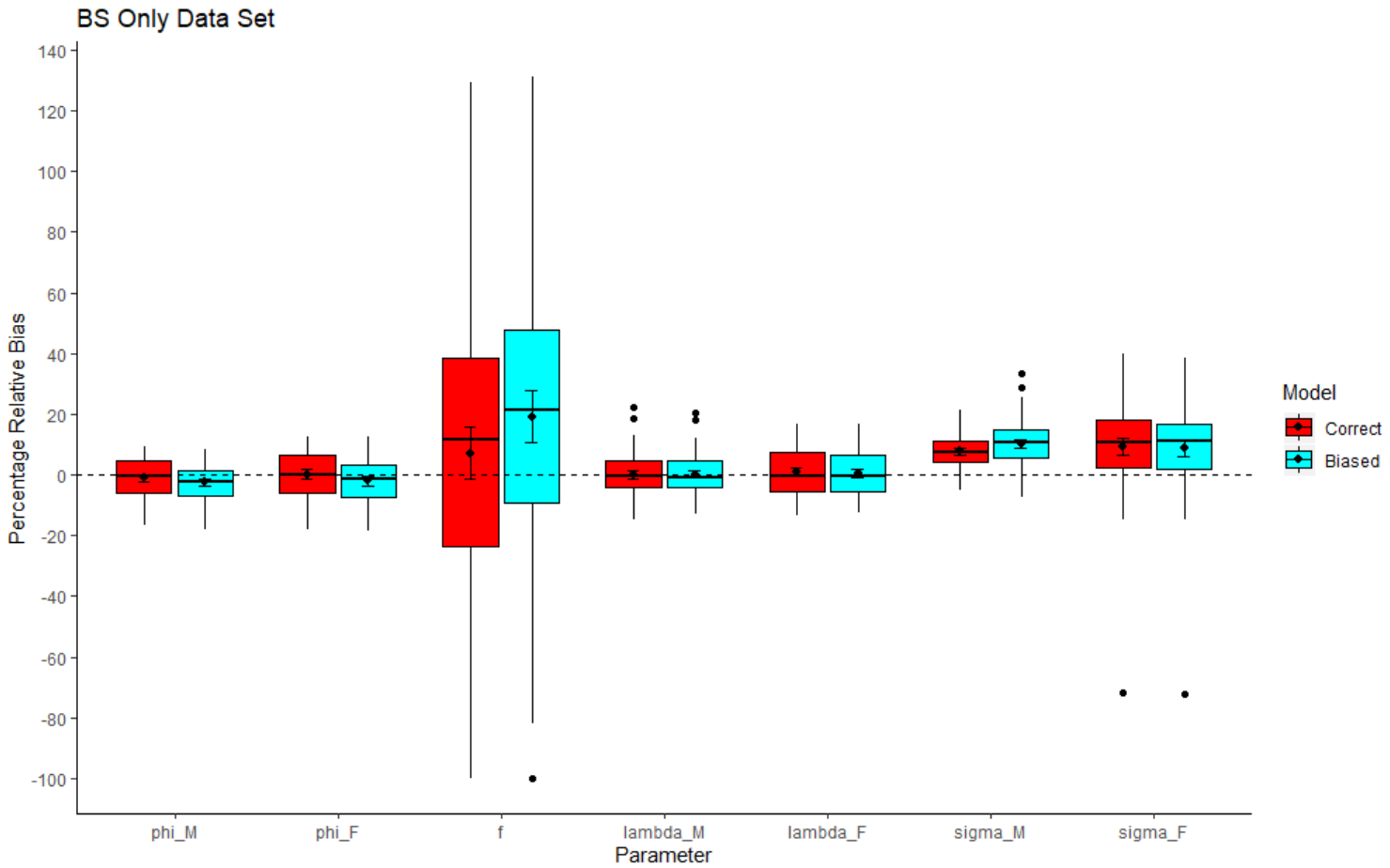

Figure 3.8. **Standard boxplots of percentage relative bias (PRB) for each parameter of interest in M_c and M_b, using only detections at BS detectors, for the λ_0 – Large simulated scenario. Whiskers extend a distance of 1.5 time the inter-quartile range from the median. Sample mean PRB along with corresponding 95% confidence intervals are also included. The results from 100 rounds of simulation were included in this figure.**

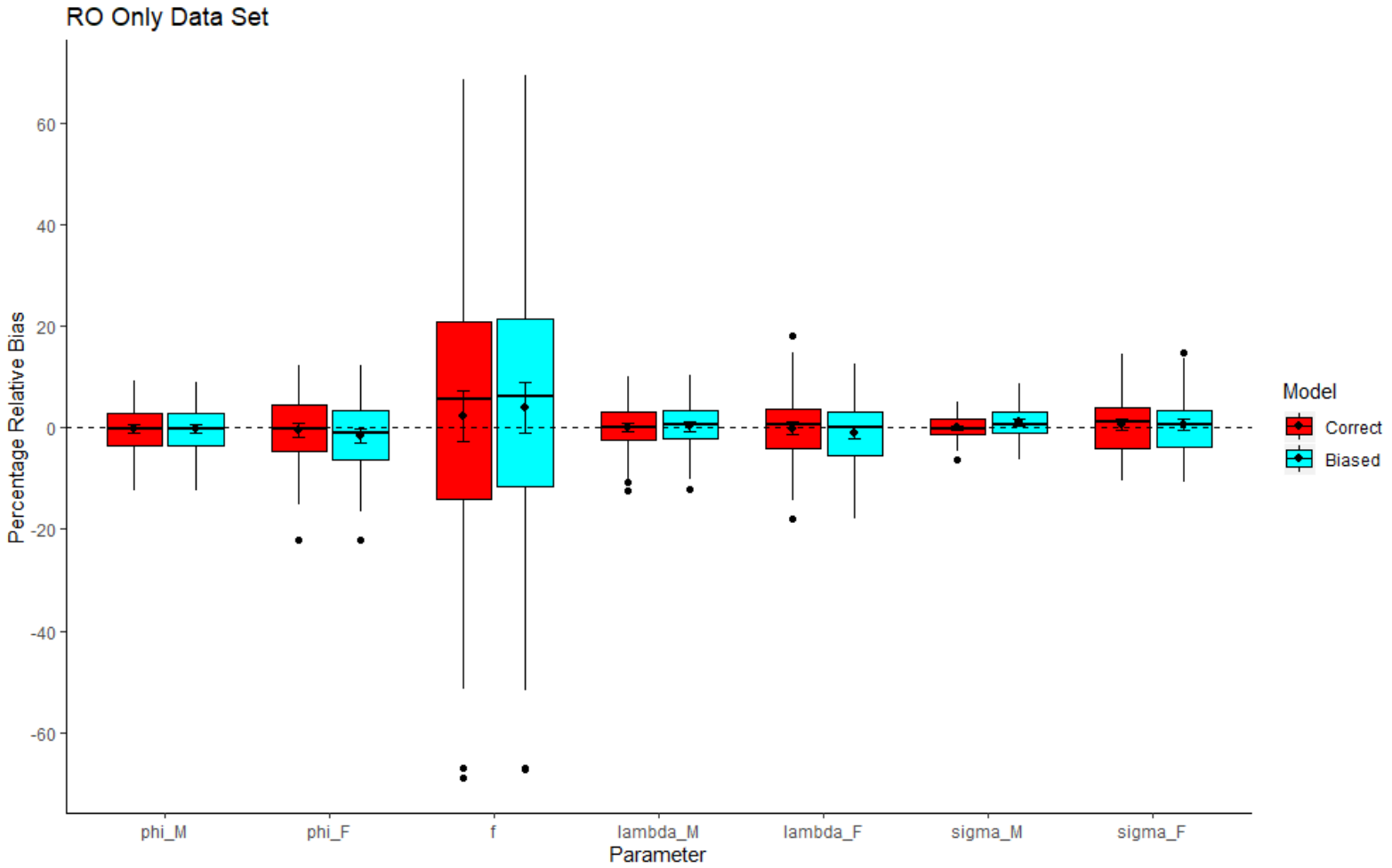

Figure 3.9. **Standard boxplots of percentage relative bias (PRB) for each parameter of interest in M_c and M_b, using only detections at RO detectors, for the λ_0 – Large simulated scenario. Whiskers extend a distance of 1.5 time the inter-quartile range from the median. Sample mean PRB along with corresponding 95% confidence intervals are also included. The results from 100 rounds of simulation were included in this figure.**

Table 3.3. Sample root mean squared error (RMSE) values for each parameter of interest in M_c and M_b, along with their ratio, for the λ_0 – Large simulated scenario using the full simulated data.

Parameter	Simulation Value	RMSE (M_c)	RMSE (M_b)	RMSE (M_b)/RMSE (M_c)
f	0.12	0.0361	0.0342	0.949
$\lambda_{Females}$	1.01	0.0628	0.0624	0.993
λ_{Males}	0.96	0.0517	0.0468	0.905
$\phi_{Females}$	0.89	0.0679	0.0657	0.967
ϕ_{Males}	0.84	0.0375	0.0357	0.952
$\sigma_{Females}$	3634	246.228	312.455	1.269
σ_{Males}	9970	297.882	426.894	1.433

Figure 3.7 shows the distribution of PRB for parameters, for models fit to the full set of detection histories, in the third simulated scenario. There are biases that seem to be introduced by M_b, however they differ somewhat from those in the previous two scenarios, possibly in part because the pattern of RO λ_0 values changed dramatically between the second and third simulation study (see Tables 2.2 and 2.3). Particularly, M_b appeared noticeably biased in estimates of $\phi_{Females}$ (Mean PRB $= -4.0\%$), $\lambda_{Females}$ (Mean PRB $= -2.1\%$), λ_{Males} (Mean PRB $= 1.0\%$), f (Mean PRB $= 12.1\%$), σ_{Males} (Mean PRB $= 2.4\%$), and $\sigma_{Females}$ (Mean PRB $= 6.4\%$). In addition, M_c also appeared biased in estimates of $\phi_{Females}$ (Mean PRB $= -3.5\%$), f (Mean PRB $= 12.1\%$), and σ_{Males} (Mean PRB $= 0.9\%$). These three biases are likely either simulation artifacts, or the result of convergence issues; *openCR* struggled particularly in this scenario to adequately estimate λ_0.

The BS only analysis had a different bias pattern in M_b than the analysis of the full data set (see Figure 3.8). Particularly, estimates of ϕ_{Males}, $\phi_{Females}$, f, σ_{Males}, and $\sigma_{Females}$ appeared at least somewhat biased. M_c was also positively biased for $\hat{\sigma}_{Males}$, and $\hat{\sigma}_{Females}$; likely due to convergence issues. The RO analysis was almost entirely unbiased for both M_c and M_b, with the exception of $\hat{\phi}_{Females}$ and $\hat{\sigma}_{Males}$ for M_b (see Figure 3.9). This could indicate that converge issues, and subsequent biases in the full data set analysis may have been largely due to the BS detectors.

Looking at Table 3.3, except for the home-range size parameters, M_b had lower RMSE than M_c when the full data set was used. In addition, the difference in RMSE for

the home-range parameters was not especially large compared to what was observed in the previous simulation studies. This is surprising as this was the scenario where it was expected RMSE would be the most unfavourable for M_b, as a very large effect was being omitted from the model. The likely explanation for this is again convergence issues. What may have occurred is that *openCR* struggled estimating the wide-ranging λ_0 values in M_c with the data available, resulting in the convergence criterion not being met and increasing bias/variance of estimates of remaining parameters.

Chapter 4.

Discussion

4.1. Interpretation of Simulation Results

The above results provide several useful insights for the South Rockies Grizzly Bear Project. The first being that despite M_c frequently outperforming M_b in terms of RMSE (with scenario 3 being the main exception, although as mentioned above this was likely due to convergence issues) the variability of most parameter estimates tended to be roughly comparable between the two methods, and the biases introduced by M_b, with the exception of the home-range size parameters, tended to not be very large relative to the size of the parameters being estimated. This low bias was even the case in the λ_0 – Large scenario where a very large effect was being omitted from the model. Thus, this suggests that South Rockies Grizzly Bear Project estimates of survival, per-capita recruitment, and population growth rates may be robust to the likely effect of an age term in λ_0 being omitted.

The home-range size parameters, however, did have some relatively large biases introduced in several scenarios. The specific biases found in the λ_0 – Small and Moderate scenarios are the most relevant to the South Rockies Grizzly Bear Project, as the parameters in the λ_0 – Large scenario were chosen more to create a very large unaccounted effect than to produce plausible detection probabilities for the South Rockies population. PRB distributions from the first two scenarios predicted that, using the full South Rockies data set, M_b $\hat{\sigma}_{Males}$ values would likely be positively biased, and $\hat{\sigma}_{Females}$ values would potentially be negatively biased.

This positive M_b $\hat{\sigma}_{Males}$ bias was likely the result of male yearlings having much higher λ_0 values at RO in the first two simulated scenarios (and higher detection probabilities; see Table 2.2 and Figure 2.1) than other age classes. When the age term was omitted, the M_b λ_0 estimate for all males detected at RO was likely lower than the male yearling-specific λ_0 value. This resulted in $\hat{\sigma}_{Males}$ being biased upwards in order to produce reasonable detection probability estimates for yearlings. This is supported by Figures 3.3 and 3.6 showing a similar positive $\hat{\sigma}_{Males}$ bias when only RO data was used.

The negative bias in $\hat{\sigma}_{Females}$ likely had a similar explanation. At BS female yearlings had much lower λ_0 values than other age classes, especially in the second and third simulated scenarios (see Table 2.2). As a result, the M_b λ_0 estimate for all females detected at BS was likely much higher than the female yearling-specific λ_0. As a result, $\hat{\sigma}_{Females}$ was biased downwards in order to produce reasonable detection probability estimates for yearlings. This is supported by Figures 3.2 and 3.5, which show that a negative bias was likely present in $\hat{\sigma}_{Females}$ when only BS data was used.

Some telemetry analyses have been carried out on the South Rockies population, placing estimated grizzly home-range size at roughly 200 km^2 for females, and 400 km^2 for males (Clayton Lamb, personal communication, June 3, 2019). Under the Gaussian space-usage pattern assumed under a half-normal detection function, this would correspond to $\hat{\sigma}_{Females} = 3259.7$, and $\hat{\sigma}_{Males} = 4609.9$. While the telemetry estimate of $\sigma_{Females}$ is similar to that obtained when M_b was fit to South Rockies data, this was not the case for σ_{Males}, where M_b produced a much larger estimate than the telemetry analysis (see Table 2.1). As telemetry analyses are more suited to estimating home-range size, this shows that similar to the findings of this simulation study, M_b likely overestimated σ_{Males} when fit to South Rockies data. This overestimation was much larger than what was observed in this study's simulations however, and there are several reasons why this might be the case.

One reason could be that had a more accurate σ_{Males} value been used to simulate capture histories (as well as corresponding λ_0 values), higher variability in $\hat{\sigma}_{Males}$ may have been observed.

Another reason could have been there was indeed home-range centre movements in male bears which M_b did not account for. When home-range movement is unaccounted for in spatial CR models, including OSECR, this can often result in σ parameters being overestimated, and λ_0 values being underestimated (Efford & Schofield, 2019; Glennie et al., 2019). A M_b model, with an added exponential home-range centre movement term was fit to a subset of the South Rockies data set (years 2012 – 2014) and compared to a M_b model fit to the same data which did not include home-range movement. The home-range centre movement model produced estimates: $\hat{\sigma}_{Males} = 6832.7$, and $\hat{\sigma}_{Females} = 4900.5$, while the static home-range centre models produced estimates: $\hat{\sigma}_{Males} = 8789.0$, and $\hat{\sigma}_{Females} = 3522.1$. Thus, looking at this subset

provided some conflicting evidence. While including home-range centre movement likely improved σ_{Males} estimates, it also may have worsened $\sigma_{Females}$ estimates.

A third cause could be that as South Rockies bears likely do not follow the Gaussian space usage pattern assumed under a half-normal detection function (see Appendix 2.2), then assuming they did could have biased $\hat{\sigma}_{Males}$ upwards. Likely, some combination of these three reasons caused the observed bias.

Overall, this probable bias in the σ_{Males} value used for simulations likely does not discount the study's findings for the non-home-range size parameters. There are two reasons for this, the first being that if the σ_{Males} value used in simulations was biased upwards, then the male λ_0 values used in simulations were likely biased downwards as they were partially based on the $\hat{\lambda}_0$ values from OSECR models fit to the South Rockies Grizzly Bear Project data set. These $\hat{\lambda}_0$ values likely would have been deflated in order to generate semi-reasonable detection probabilities, based on the observed data, given the inflated $\hat{\sigma}_{Males}$ value. Thus, the detection probabilities used to generate simulated data may not have been too biased. Secondly, the simulation study varied λ_0 values considerably, resulting in male bear detection functions taking on many different shapes, and in all these cases, it did not appear that M_b estimates of survival, recruitment, or growth rate had been greatly biased.

The finding that M_b σ_{Males} estimates are often subject to bias is not very surprising. As detection probability is a function of both σ and λ_0, it makes sense that σ estimates may become biased to compensate for λ_0 being misspecified. Of all the parameters under consideration in this study, the home-range size parameters were of the least interest, in part because bear home-range sizes are already relatively well understood, and because there are alternative methods for estimating their size, such as telemetry analyses. Thus, this simulation study's findings are promising, as they concluded that estimates of survival, recruitment, and population growth rate are likely not being overly affected by the lack of age data in South Rockies Grizzly Bear Project data sets.

Moving on to the second question posed in this analysis, comparing the differences in BS and RO only results for the first two simulated scenarios (again, because these two scenarios contain plausible λ_0 values for the South Rockies

population) shows that both detector types tended to produce reasonably accurate parameter estimates under M_b, with the exception of $\hat{\sigma}_{Males}$ and $\hat{\sigma}_{Females}$. Both detector types showed different patterns in PRB distributions for these two parameters, with BS detectors generally producing more accurate estimates of σ_{Males}, and RO detectors producing more accurate estimates of $\sigma_{Females}$. It is difficult to determine which detector type is less prone overall to producing biased parameter estimates using these results alone, as some of the bias in BS parameter estimates may have been caused by the size of simulated detection histories. This was evidenced by PRB being much more variable in BS only analyses, as well as bias in home-range size parameters dropping noticeably in BS only analyses between the first and second simulation study, coinciding with average detection probabilities across sexes increasing.

Thus, overall it seems both detector types are prone to bias that is capable hindering M_b's ability to accurately estimate home-range size parameters. Further work would be required to determine which type of detector produces the best parameter estimates relative to a performance metric such as RMSE, within the context and budget of the South Rockies project.

4.2. Future Work

There are several avenues for future work on this problem. These mainly centre on modifying the simulation procedure to be more realistic. For example, as mentioned in Section 2.3, there are likely other OSECR parameters that could be modelled as a function of age, such as survival and home-range size: Younger males likely have lower survival rates than older males, yearling home-range size is likely very similar to adult female home-range sizes as they follow them around, etc. Further work could be done to determine reasonable values for these effects and incorporate them.

Similarly, home-range centre movement models (especially ones that model home-range centre movement as a function of sex) should be further explored, as there is evidence (see Section 4.4 and Appendix 2.2) that this is occurring in South Rockies data. Once these models have been examined, home-range centre movement could be added to simulations and be included in M_c and M_b models used to evaluate PRB.

The main hurdle for implementing these changes to the simulation procedure would be controlling computation time. The results of this simulation study showed that to avoid convergence issues in *openCR*'s default algorithm, a larger simulated data set is likely required. This would be especially true if further model complexity was introduced. Data set size could be increased by deploying more detectors over a larger region, or simulating additional primary/secondary sampling occasions. Doing either of these would likely cause issues though, as simulating more data, as well as increasing model complexity, both have the potential to greatly increase computation time. Thus, before attempting this with *openCR*, other packages that use frequentist methods to quickly estimate parameters from open, spatial CR models, such as *openpopscr* (Glennie et al., 2019), or *oSCR* (Sutherland, Royle, & Linden, 2018) should be explored to see if they can reduce computation time.

Many other forms of data have been collected in the South Rockies Grizzly Bear Project, such as telemetry data, and incidental bear sightings. Further analyzing these data sets, as well as researching models that can directly incorporate this data in models along with the CR data could also prove enlightening.

Chapter 5.

Conclusion

Under the models examined in this paper, it is likely that South Rockies Grizzly Bear Project OSECR estimates of apparent year-to-year survival, apparent per-capita recruitment, and population growth rate have only a small bias when grizzly bear age class (yearling, sub-adult, or adult) is not included in the λ_0 portion of the half-normal detection probability function. This was not the case for estimates of the male and female home-range size parameters though (and especially so for the male parameter), which were biased in several of the simulated scenarios examined. In addition, it was found that while both detector types tended to produce low-bias estimates of survival, recruitment, and population growth when M_b was used, they also often produced noticeably biased estimates of home-range size parameters. In the case of BS detectors, this may have been in part caused by the simulated sample size being too small. Finally, this study also found that the default maximization algorithm in the *openCR* package can struggle with convergence issues when there are very large class differences in λ_0 values, and that larger simulated data sets may need to be employed in future studies to account for this.

References

Akaike, H. (1974). A New Look at the Statistical Model Identification. IEEE Transactions on Automatic Control, 19(6), 716–723. https://doi.org/10.1109/TAC.1974.1100705

Borchers, D. L., & Efford, M. G. (2008). Spatially explicit maximum likelihood methods for capture-recapture studies. Biometrics, 64(2), 377–385. https://doi.org/10.1111/j.1541-0420.2007.00927.x

Boulanger, J., Stenhouse, G., & Munro, R. (2004). Sources of Heterogeneity Bias When Dna Mark-Recapture Sampling Methods Are Applied To Grizzly Bear (Ursus Arctos) Populations. Journal of Mammalogy, 85(4), 618–624. https://doi.org/10.1644/brb-134

Chapman, D. G., Otis, D. L., Burnham, K. P., White, G. C., & Anderson, D. R. (1978). Statistical Inference from Capture Data on Closed Animal Populations. Populations. Wildlife Monographs, 62, 3-135.

Clapham, M., Nevin, O. T., Ramsey, A. D., & Rosell, F. (2012). A hypothetico-deductive approach to assessing the social function of chemical signalling in a non-territorial solitary carnivore. PLoS ONE, 7(4). https://doi.org/10.1371/journal.pone.0035404

Clapham, M., Nevin, O. T., Ramsey, A. D., & Rosell, F. (2014). Scent-marking investment and motor patterns are affected by the age and sex of wild brown bears. Animal Behaviour, 94, 107–116. https://doi.org/10.1016/j.anbehav.2014.05.017

Efford, M. G. (2014). Bias from heterogeneous usage of space in spatially explicit capture-recapture analyses. Methods in Ecology and Evolution, 5(7), 599–602. https://doi.org/10.1111/2041-210X.12169

Efford, M. G. (2019). openCR: Open population capture-recapture models. R package version 1.4.1. https://CRAN.R-project.org/package=openCR

Efford, M. G., Borchers, D. L., & Mowat, G. (2013). Varying effort in capture-recapture studies. Methods in Ecology and Evolution, 4(7), 629–636. https://doi.org/10.1111/2041-210X.12049

Efford, M. G., & Schofield, M. R. (2019). A spatial open-population capture-recapture model. Biometrics. https://doi.org/10.1111/biom.13150

Gardner, B., Reppucci, J., Lucherini, M., & Royle, J. A. (2010). Spatially explicit inference for open populations: Estimating demographic parameters from camera-trap studies. Ecology, 91(11), 3376–3383. https://doi.org/10.1890/09-0804.1

Glennie, R., Borchers, D. L., Murchie, M., Harmsen, B. J., & Foster, R. J. (2019). Open population maximum likelihood spatial capture-recapture. Biometrics, 75(4), 1345-1355. https://doi.org/10.1111/biom.13078

Haroldson, M. A., Ternent, M. A., Gunther, K. A., & Schwartz, C. C. (2002). Grizzly bear denning chronology and movements in the Greater Yellowstone ecosystem. Ursus, 13, 29–37.

Kendall, K. C., Stetz, J. B., Boulanger, J., Macleod, A. C., Paetkau, D., & White, G. C. (2009). Demography and Genetic Structure of a Recovering Grizzly Bear Population. Journal of Wildlife Management, 73(1), 3–17. https://doi.org/10.2193/2008-330

Lamb, C. T., Ford, A. T., Proctor, M. F., Royle, J. A., Mowat, G., & Boutin, S. (2019). Genetic tagging in the Anthropocene: scaling ecology from alleles to ecosystems. Ecological Applications, 29(4), 1–17. https://doi.org/10.1002/eap.1876

Lamb, C. T., Mowat, G., McLellan, B. N., Nielsen, S. E., & Boutin, S. (2017). Forbidden fruit: human settlement and abundant fruit create an ecological trap for an apex omnivore. Journal of Animal Ecology, 86(1), 55–65. https://doi.org/10.1111/1365-2656.12589

Lamb, C. T., Walsh, D. A., & Mowat, G. (2016). Factors influencing detection of grizzly bears at genetic sampling sites. Ursus, 27(1), 31. https://doi.org/10.2192/ursus-d-15-00025.1

Link, W. A., & Barker, R. J. (2005). Modeling association among demographic parameters in analysis of open population capture-recapture data. Biometrics, 61(1), 46–54. https://doi.org/10.1111/j.0006-341X.2005.030906.x

McLellan, B. N. (1989). Dynamics of a grizzly bear population during a period of industrial resource extraction. I. Density and age-sex composition. Canadian Journal of Zoology, 67(8), 1856–1860. https://doi.org/10.1139/z89-264

Mowat, G., Heard, D. C., Seip, D. R., Poole, K. G., Stenhouse, G., & Paetkau, D. W. (2005). Grizzly Ursus arctos and black bear U. americanus densities in the interior mountains of North America. Wildlife Biology, 11(1), 31–48. https://doi.org/10.2981/0909-6396

Paetkau, D. (2003). An empirical exploration of data quality in DNA-based population inventories. Molecular Ecology, 12(6), 1375–1387. https://doi.org/10.1046/j.1365-294X.2003.01820.x

Pledger, S., Pollock, K. H., & Norris, J. L. (2010). Open capture-recapture models with heterogeneity: II. Jolly-Seber model. Biometrics, 66(3), 883–890. https://doi.org/10.1111/j.1541-0420.2009.01361.x

Pollock, K. H. (1982). A Capture-Recapture Design Robust to Unequal Probability of Capture. The Journal of Wildlife Management, 46(3), 752. https://doi.org/10.2307/3808568

Pradel, R. (1996). Utilization of Capture-Mark-Recapture for the Study of Recruitment and Population Growth Rate. Biometrics, 52(2), 703. https://doi.org/10.2307/2532908

R Core Team. (2019). R: A Language and Environment for Statistical Computing. Vienna, Austria: R Foundation for Statistical Computing. https://www.r-project.org/

Robert, C. P. (2004). Monte Carlo statistical methods / Christian P. Robert, George Casella. New York, NY: Springer Press.

Royle, J. A., Chandler, R. B., Sollmann, R., & Gardner, B. (2014). Spatial capture-recapture. Waltham, MA: Academic Press.

Schofield, M. R., & Barker, R. J. (2008). A unified capture-recapture framework. Journal of Agricultural, Biological, and Environmental Statistics, 13(4), 458–477. https://doi.org/10.1198/108571108X383465

Schwarz, C. J., & Arnason, A. N. (1996). A General Methodology for the Analysis of Capture-Recapture Experiments in Open Populations. Biometrics, 52(3), 860. https://doi.org/10.2307/2533048

Sutherland, C., Royle, A., & Linden, D. (2018). oSCR: Multi-Session Sex-Structured Spatial Capture-Recapture Models. R package version 0.42.0

Appendix 1.

Relevant Capture-Recapture Models

The OSECR model, introduced in Efford & Schofield (2019), can be thought of as a combination of two well-known CR models: The non-spatial, open population model of Schwarz & Arnason (1996), referred to here as JSSA, and the spatially explicit, closed population model of Borchers & Efford (2008), hence referred to as SECR. These two models will be examined in further detail before OSECR is.

Appendix 1.1: JSSA

In studies using the JSSA model, each detected animal's detection history is a string of 1's and 0's, indicating whether that animal was detected at any of the detectors on a given secondary sampling occasion. Individual i's JSSA detection history will be denoted as ω_i'. For example, if a study was conducted with 4 primary occasions, each one having a single secondary occasion, a detection history of $\omega_i' = \mathbf{0110}$ would indicate animal i was not detected during the first, and fourth primary occasions, but was on the second and third. Animals that were not detected are assumed to have detection histories of all zeros. Note that in order to use this form of the JSSA, you must have a method of individually identifying or marking animals, so that each animal can be assigned a unique detection history. These detection histories are used as inputs in the JSSA model, which has a likelihood of the form: $L(\theta, N|\omega') = \Pr(n|\theta, N)\Pr(\omega'|n, \theta)$, where ω' is the set of observed detection histories, n is the number of individual animals detected, N is a superpopulation parameter representing the number of unique animals available for detection in the population over the study period, and θ is a list of detection and population dynamics parameters which will be explained below.

Treating n as a binomial random variable, the first component of the JSSA's likelihood is expressed as: $\Pr(n|\theta, N) = \binom{N}{n} p^n (1-p)^{N-n}$, where p is the probability that an animal from the super population N is detected at least once over the course of the study. The second component of the likelihood has the form: $\Pr(\omega'|n, \theta) \propto \prod_{\omega_i' \in \omega'} \Pr(\omega_i'|\omega_i' > 0)$, where $\Pr(\omega_i'|\omega_i' > 0)$ represents the probability of observing detection history ω_i', conditional on the animal being detected at all during the study.

Using the individual-based notation of Link & Barker (2005) and Schofield & Barker (2008), $\Pr(\omega_i'|\omega_i' > 0)$ is expressed as:

$$\Pr(\omega_i'|\omega_i' > 0) = \sum_{b=1}^{f_i} \sum_{d=l_i}^{J} \Pr(b,d) \Pr(\omega_i'|b,d,\omega_i' > 0) \qquad (A1-1),$$

where f_i is the primary occasion where animal i was first detected, and l_i is the last primary occasion where animal i was detected.

$\Pr(b,d)$ is the probability that an animal was first available for detection at primary occasion b (either because the animal was already in the population of interest if $b = 1$, or because the animal subsequently entered the population through birth or immigration if $b > 1$), and was last available for detection at primary occasion d (either because the animal died, or emigrated from the population after occasion d). This probability can be parameterized as $\Pr(b,d) = \beta_{b-1}(\prod_{j=b}^{d-1}\phi_j)(1-\phi_d)$, where β_j represents the probability that an animal from superpopulation N first became available to be detected at primary occasion $j+1$. These β parameters are often referred to as entrance probabilities. ϕ_j represents the probability that an animal available for detection at primary occasion j remained available for detection at primary occasion $j+1$ (i.e. because it did not die, or permanently emigrate after primary occasion j). These ϕ parameters are usually called apparent survival rates. The term "apparent" is used because this model does not distinguish between animals that died, and animals that simply left the study area permanently.

As an example, we'll return to the $\omega_i' = \mathbf{0110}$ detection history. In this example, $f_i = 2$, and $l_i = 3$. See the third column of Table A1.1 for all the possible $\Pr(b,d)$ values for this scenario.

Table A1.1 All possible $Pr\ (b,d)$ and $\Pr(\omega_i'|b,d,\omega_i' > 0)$ values under the JSSA model for the detection history $\omega_i' = 0110$.

b	d	$\Pr(b,d)$	$\Pr(\omega_i'\|b,d,\omega_i' > 0)$
1	3	$\beta_0\phi_1\phi_2(1-\phi_3)$	$p_\cdot^{-1}(1-p_1)p_2p_3$
1	4	$\beta_0\phi_1\phi_2\phi_3$	$p_\cdot^{-1}(1-p_1)p_2p_3(1-p_4)$
2	3	$\beta_1\phi_2(1-\phi_3)$	$p_\cdot^{-1}p_2p_3$
2	4	$\beta_1\phi_2\phi_3$	$p_\cdot^{-1}p_2p_3(1-p_4)$

The second component of equation (A1 – 1) has the form:

$$\Pr\left(\omega_i' | b, d, \omega_i' > 0\right) = p_{\cdot}^{-1} \prod_{j=b}^{d} \prod_{k=1}^{K_j} p_{j,k}^{\omega'_{ijk}} \left(1 - p_{j,k}\right)^{1-\omega'_{ijk}}.$$

$p_{j,k}$ is the probability an animal is detected on secondary occasion k of primary occasion j, assuming the animal was available for detection then. ω'_{ijk} is animal i's detection history for secondary occasion k of primary occasion j (i.e. $\omega'_{ijk} = 1$ if the animal was detected on that secondary occasion, $\omega'_{ijk} = 0$ otherwise). $p_{\cdot}$ represents the probability that an animal is detected at all during the study period, and is expressed as $p_{\cdot} = 1 - \sum_{b=1}^{J} \sum_{d=b}^{J} \left\{ \Pr(b, d) \prod_{j=b}^{d} \prod_{k=1}^{K_j} \left(1 - p_{j,k}\right) \right\}$.

Using the above parameterization of the JSSA, it is possible to estimate primary occasion-specific population sizes using $\hat{\beta}_j$ and $\hat{\phi}_j$ values. Alternatively, they can also be calculated using the Horvitz-Thompson style estimator: $N_j = \sum_{i=1}^{n} \hat{p}_{i,j}^{-1} * I(i \in n_j)$, where $I\left(i \in n_j\right) = 1$ if animal i was detected in primary occasion j, and 0 otherwise. $\hat{p}_{i,j}$ represents the model estimated probability of detecting animal i during primary occasion j and can be written as $\hat{p}_{i,j} = 1 - \sum_{k=1}^{K_j} (1 - \hat{p}_{j,k})$.

Conceptually, the notion of parameterizing the JSSA likelihood with entry probabilities β_j is straightforward; however, these probabilities do not have clear biological interpretations, and do not lend themselves to explaining the dynamics of a population. As a result, several different parameterizations of the JSSA likelihood have been derived (Efford & Schofield, 2019; Pradel, 1996; Schwarz & Arnason, 1996). A commonly used parameterization explored in this paper is the Pradel-Link-Barker (PLB) formulation (Link & Barker, 2005; Pradel, 1996). In the PLB parameterization, the entry probabilities β_j are replaced with per-capita recruitment probabilities f_j, which represents how many new animals enter the population between primary occasions j and $j + 1$ and are still alive at primary occasion $j + 1$, per animal currently alive at primary occasion j.

It is possible to first fit the JSSA model described above, and then recursively calculate the f_j parameters, using the following relationships shown in Link & Barker (2005): $d_{j+1} = d_j \phi_j + \beta_j$ (where $d_1 = \beta_0$), and $f_j = \beta_j / d_j$. Examining the form of d_{j+1}, it

represents the proportion of the super-population that is alive during primary occasion $j + 1$. Thus, β_j/d_j is the ratio of the portion of the super-population that became available for sampling in primary occasion $j + 1$, and the portion of the super-population alive at primary occasion j, which is equivalent to the definition of per-capita recruitment probabilities described above. In addition, Link & Barker (2005) also provides an alternative likelihood parameterization that directly uses f_j instead of β_j. If this form is used, β_j can be derived recursively. It should be noted that the PLB formulation is a conditional CR model: Its likelihood has the form $L(\theta, N|\omega') = \Pr(\omega'|n, \theta)$, and does not contain a super-population parameter. In this case, the super-population parameter can be calculated using the Horvitz-Thompson style estimator: $\widehat{N} = \sum_{i=1}^{n} \hat{p}_i^{-1}$, where $\hat{p}_i$ is the estimated probability that animal i was detected at least once over the course of the study. Primary occasion-specific population estimates can be derived in the same way as in the JSSA model.

In the JSSA model, N is parameterized on the log scale, while the parameters p, $p_{j,k}$, and ϕ_j are parameterized on the logit scale. This is to ensure the estimated super-population is positive, and the parameters which represent probabilities are bounded between 0 and 1. In the PLB parameterization, f_j is on the log scale. These parameters can be modelled as linear combinations of covariates in their respective link scales in a straightforward manner.

One issue with JSSA/PLB abundance estimates is that unless the study region is a thoroughly sampled, geographically closed region, such as a pond, there is no way to know exactly what region estimates of abundance corresponds to. As a result, there is no clear method of estimating population density (which could then be used to estimate abundance in a region of interest). There are a number of ad-hoc methods that have been developed to estimate density, but this issue can also be directly resolved by using spatially explicit CR methods (Borchers & Efford, 2008; Royle et al., 2014)

The JSSA/PLB models have a number of assumptions:

- Animals are detected independently of one-another, i.e. $\Pr(\omega'|n, \theta) \propto \prod_{\omega_i' \in \omega'} \Pr(\omega_i'|\omega_i' > 0)$.
- Detections within an individual animal, across sampling occasions, are independent, i.e. $\Pr(\omega_i'|b, d, \omega_i' > 0) = p_{\cdot}^{-1} \prod_{j=b}^{d} \prod_{k=1}^{K_j} p_{j,k}^{\omega'_{ijk}} \left(1 - p_{j,k}\right)^{1-\omega'_{ijk}}$.

- Animals remain individually identifiable over the course of the study.
- The study area remains consistent over the entire study.
- Detection probability, year-to-year survival, and per-capita recruitment are the same for both detected and undetected animals who share the same covariate values.
- Animals do not die in the detection process.
- Once an animal has left the population, it cannot return, i.e. animals do not temporarily emigrate.

Appendix 1.2: SECR

SECR is a spatially explicit, closed CR method. It assumes that there is no population turnover between primary occasions, and that the probability of detecting an animal at a detector is in part a function of what areas in the study region an animal occupies. SECR is parameterized in such a way that it can directly generate population density estimates.

Like JSSA models, it is assumed the study has J primary sampling occasions, each with K_j secondary sampling occasions. A series of S_j detectors are deployed each primary occasion, with detector s located at Cartesian coordinate t_s. There are assumed to be n unique animals caught. Each animal is assumed to have a "home-range centre", $\boldsymbol{X}$, located at Cartesian coordinate x_i. Royle et al. (2014) defined an animal's home-range centre as "The centroid of the space that individual occupied (or used) during the period in which traps [detectors] were active". $\boldsymbol{X}$ is not directly observable. SECR assumes home-range centres are independent and are generated by an inhomogeneous Poisson process with rate parameter $D(\mathbf{X}; \tau)$, were τ is a vector of parameters governing the Poisson process.

The set of detection histories for a SECR study is represented as ω, with ω_i referring to animal i's individual detection history. ω_i can be thought of as a collection of J, $S_j \times K_j$ matrices, with matrix j having a value of 1 in element (s, k) if animal i was detected at detector s during secondary occasion k of primary occasion j, and 0 if it was not detected then. Note that depending on the type of detector used, the matrices in ω_i can contain different values. For example, there are SECR formulations that take as inputs the number of times an individual was detected at a detector over the course of a

secondary occasion. When acoustic sensors are used, SECR models can take the amplitude of animal noises detected as input. This paper will focus on the binary form of ω_i described first, as this was how data in the South Rockies Grizzly Bear Project were summarized.

It is assumed the probability of an animal being captured at detector s during secondary occasion k of primary occasion j governed by the detection function $p_{jks}(\mathbf{X};\theta)$, where θ is a vector of detection probability parameters. There are a number of detection functions that can be used in CR studies (Borchers & Efford, 2008; Royle et al., 2014). The most commonly used detection function, which will be used in this paper, is the half-normal detection function:

$$p_{jks} = \lambda_0 \exp\left(-\frac{1}{2\sigma^2}\|\mathbf{X} - t_s\|^2\right) \qquad (A1-2),$$

where λ_0 can be interpreted as the probability of detecting an animal at a detector located at t_s, and σ can be thought of as a home-range size parameter, with larger values of σ corresponding to larger home-range sizes. σ will be discussed further below.

The detection function selected dictates what space usage model is assumed of animals in a study. For instance, choosing the half-normal detection function implies a bivariate normal model of space use, where the probability of an animal using a point on the habitat grid can be modelled as coming from a circular bivariate Gaussian distribution with standard deviation σ (the same σ as in equation A1 – 2). This clarifies how the σ parameter in equation A1 – 2 is directly linked with home-range size.

The SECR likelihood can be written as

$$\mathrm{L}(\tau, \theta \mid n, \omega) = \Pr(n \mid \tau, \theta)\Pr(\omega \mid n, \theta, \tau) \qquad (A1-3).$$

If it is assumed that detection probabilities are independent between animals, then the first component of equation A1 – 3, $\Pr(n \mid \tau, \theta)$, is a Poisson probability density function with rate parameter $\delta(\tau, \theta) = \int_{\mathcal{R}^2} D(\mathbf{X};\tau)p_{\cdot}(\mathbf{X};\theta)d\mathbf{X}$, where $p_{\cdot}(x_i;\theta)$ is the probability that an animal with home-range centre $\boldsymbol{X}$ is detected at least once over the course of the study period. Using the half-normal detection function, and assuming that detections within animals are independent, $p_{\cdot}(\mathbf{X};\theta) = 1 - \prod_{j=1}^{J}\prod_{k=1}^{K_j}\prod_{s=1}^{S_j}\left(1 -\right.$

$p_{jks}(\mathbf{X};\theta)\Big)$. This equation for the rate parameter makes intuitive sense. As the Poisson process $D(\mathbf{X};\tau)$ parameterizes the density of animals at each point in $\mathcal{R}^2$, and $p_{\cdot}(\mathbf{X};\theta)$ parameterizes the probability of detecting an animal at each point in $\mathcal{R}^2$, the integral of their product would give the expected number of detected animals.

The second component of equation A1 – 3, $\Pr(\omega \mid n,\theta,\tau)$, is expressed as $\Pr(\omega \mid n,\theta,\tau) \propto \prod_{i=1}^{n} \Pr(\omega_i \mid \omega_i > 0,\tau,\theta)$, where $\omega_i > 0$ indicates animal i was detected at least once in the study. The likelihood of each animal's detection history, conditional on it being detected, can in turn be written as

$$\Pr(\omega_i \mid \omega_i > 0,\tau,\theta) = \int_{\mathcal{R}^2} \Pr(\omega_i \mid \omega_i > 0,\tau,\theta,\mathbf{X}) f(\mathbf{X} \mid \omega_i > 0,\tau,\theta) d\mathbf{X} \qquad (A1-4),$$

where

$$f(\mathbf{X} \mid \omega_i > 0,\tau,\theta) = D(\mathbf{X};\tau)p_{\cdot}(\mathbf{X};\theta) \Big/ \int_{\mathcal{R}^2} D(\mathbf{X};\tau)p_{\cdot}(\mathbf{X};\theta)dx_i$$

$$= D(\mathbf{X};\tau)p_{\cdot}(\mathbf{X};\theta) \Big/ \delta(\tau,\theta),$$

is the probability density function of animal i's home-range centre, conditional on it being detected.

The probability of a detection history, conditional on home-range centre $\boldsymbol{X}$, and the animal being detected, can be written as $\Pr(\omega_i \mid \omega_i > 0,\tau,\theta,\mathbf{X}) = p_{\cdot}(\mathbf{X})^{-1} \prod_{j=1}^{J} \prod_{k=1}^{K_j} \prod_{s=1}^{S_j} p_{jks}{}^{\omega_{ijks}} (1-p_{jks})^{1-\omega_{ijks}}$, where $\omega_{ijks} = 1$ if animal i was detected at detector s on secondary occasion k of primary occasion j, and 0 otherwise.

Thus, because the probability of detecting an animal is a function of its home-range centre, which is unobserved, to calculate the marginal likelihood of a detection history one must integrate over all possible home-range centres.

Using the maximum likelihood estimate of τ, it is possible to estimate density at locations of interest using $\widehat{D}(\mathbf{X};\hat{\tau})$. Region-specific densities can be estimated using $\frac{\int_A \widehat{D}(\mathbf{X};\hat{\tau})d\mathbf{X}}{\|A\|}$, where A is a region of interest with area $\|A\|$.

In the case when the Poisson process generating home-range centres is homogeneous (i.e., population density is assumed constant), with rate parameter D, then equation A1 – 3 can be rewritten as

$$\mathrm{L}(\theta, \mathrm{D} \mid n, \omega) \propto \frac{[Da(\theta)]^n \exp\left(-Da(\theta)\right)}{n!} \times \prod_{i=1}^{n} \frac{\int \Pr(\omega_i \mid \mathbf{X}; \theta) d\mathbf{X}}{a(\theta)} \qquad (A1-5),$$

where $\Pr(\omega_i \mid \mathbf{X}; \theta) = \prod_{j=1}^{J} \prod_{k=1}^{K_j} \prod_{s=1}^{S_j} {p_{jks}}^{\omega_{ijks}} (1 - {p_{jks}}^{1-\omega_{ijks}})$, and $a(\theta) = \int p_{\cdot}(\mathbf{X}; \theta)$. When this homogeneity is assumed, it is possible to estimate detection parameters θ separate from D, using the conditional model $L(\theta \mid n, \omega) \propto \prod_{i=1}^{n} \frac{\int \Pr(\omega_i \mid \mathbf{X}; \theta) d\mathbf{X}}{a(\theta)}$. The maximum likelihood estimates from this conditional model are identical to those of the full model in equation A1 – 5 (Borchers & Efford, 2008). Under the conditional model, density must be estimated using the Horvitz-Thompson style estimator $\widehat{D} = \sum_{i=1}^{n} \hat{a}(z_i)^{-1}$, where z_i are any covariates for detection probability which may be in the model (see below). This conditional model is analogous to the JSSA conditional model discussed previously.

The detection parameters λ_0 and σ are typically parameterized using logit and log links respectively, and both can be parameterized as linear functions of covariates on their link scales. Population density for a given point in space, $D(\mathbf{X}; \tau)$, is typically parameterized using a log link, and can similarly be treated as a linear function of covariates on the log scale. Note that in order to model density as a function of covariates (thus assuming inhomogeneous density) the full likelihood model must be used.

While the Poisson process $D(\mathbf{X}; \tau)$ was first described parameterizing density over $\mathcal{R}^2$, in practice this area of integration can be reduced substantially, as after a certain distance detection probability essentially drops to 0 under the half-normal detection function (as well as most other commonly used detection functions). The area of integration should be selected by the SECR user, taking into account how large the home-ranges of the species under consideration are thought to be. Also note that any non-habitat area in a study region where it is highly unlikely a home-range centre would occur can also be removed from the area of integration.

In CR studies certain detectors may only be deployed for a subset of secondary occasions within a primary occasion, or are left out longer than others. Both the full and conditional SECR likelihoods can be modified to accommodate these possibilities. In the first case, the Bernoulli terms in $\Pr(\omega_i \mid \omega_i > 0, \tau, \theta, \mathbf{X}) = p_{\cdot}(\mathbf{X})^{-1} \prod_{j=1}^{J} \prod_{k=1}^{K_j} \prod_{s=1}^{S_j} {p_{jks}}^{\omega_{ijks}} (1 - p_{jks})^{1-\omega_{ijks}}$ that correspond to the occasions a detector wasn't deployed can simply be replaced by 1. Addressing the second case is dependent on the type of detectors used. For binary detectors, this can be addressed by replacing the p_{jks} terms in $\Pr(\omega_i \mid \omega_i > 0, \tau, \theta, \mathbf{X})$ with $g_{jks} = 1 - (1 - p_{jks})^{T_{sk}}$, where T_{sk} is the amount of time a detector was deployed for (often in days) (Efford et al., 2013). In this case the half-normal detection function parameter λ_0 should be interpreted as the probability of detecting an animal over a single time unit when its home range centre lines up with a detector's location.

The SECR model has several assumptions, some of which have already been mentioned in passing:

- There is no population turnover for the duration of the study.
- Detection probabilities are independent between animals.
- Detection probabilities are independent within animals.
- Animals remain individually identifiable throughout the study period.
- There is no death on detection.

Note that the JSSA assumption that the study area remains constant can be relaxed in SECR. As long as the area of integration is large enough to encompass all the feasible home-range centres, based on the detectors deployed in the study, then the region in which detectors are deployed is free to vary between primary or secondary occasions. In addition, the assumption that animals with identical covariate values have the same detection probability has also been relaxed, as detection probability is allowed to vary with home-range centre location.

Appendix 1.3: OSECR

The OSECR model derived by Efford & Schofield (2019) is a spatiotemporal CR model that is spatially explicit, while also allowing for population turnover. Efford &

Schofield (2019) derived two forms of OSECR, one where home-range centres are assumed stationary throughout the study period, and one where they are modeled as moving between primary sampling occasions. This paper will focus on the stationary model. For convenience, OSECR will refer to the stationary home-range centre OSECR model.

When home-range centres are assumed stationary, OSECR adapts the JSSA model to be spatially explicit, borrowing parts of SECR's functional form. OSECR essentially replaces the JSSA detection model from equation A1 – 1: $p_{\cdot}^{-1}\prod_{j=b}^{d}\prod_{k=1}^{K_j} p_{j,k}^{\omega'_{ijk}}\left(1-p_{j,k}\right)^{1-\omega'_{ijk}}$, with the SECR detection model from equation A1 – 4: $\int_{\mathcal{R}^2} p_{\cdot}(\mathbf{X})^{-1}\prod_{j=1}^{J}\prod_{k=1}^{K_j}\prod_{s=1}^{S_j} p_{jks}{}^{\omega_{ijks}}(1-p_{jks})^{1-\omega_{ijks}} f(\mathbf{X}|\ \omega_i>0,\tau,\theta)d\mathbf{X}$. Secondly, it parameterizes the JSSA super-population as a collection of animal home-range centres that are generated by an inhomogeneous Poisson point process, $D(\boldsymbol{X};\tau)$, over $\mathcal{R}^2$.

The OSECR likelihood has the familiar $\mathrm{L}(\tau,\theta\mid n,\omega)=\Pr(n\mid\ \tau,\theta)\Pr(\omega\mid\ n,\theta,\tau)$ form. This likelihood's first component, $\Pr(n\mid\ \tau,\theta)$, is modelled as a Poisson density, with rate parameter $\delta=\ \sum_{b=1}^{J}\sum_{d=b}^{J}\Pr\ (b,d)\int p_{\cdot}(\boldsymbol{X}|\ b,d)D(\boldsymbol{X};\tau)d\boldsymbol{X}$, where $\Pr\ (b,d)$ is the same as in the JSSA model, and $p_{\cdot}(\boldsymbol{X}|\ b,d)$ is equivalent to $p_{\cdot}(\boldsymbol{X})$ from SECR, modified for the animal first being available for detection at primary occasion b, and last available for detection at primary occasion d: $p_{\cdot}(\boldsymbol{X};b,d)=1-\ \prod_{j=b}^{d}\prod_{k=1}^{K_j}\prod_{s=1}^{S_j}\left(1-p_{jks}(\boldsymbol{X};\theta)\right)$.

The second component of the above likelihood has the form

$$\Pr(\omega\mid\ n,\theta,\tau)\ \propto\ \prod_{\omega_i\in\omega}\sum_{b=1}^{f_i}\sum_{d=\ l_i}^{J}\Pr(b,d)\Pr(\omega_i\mid\ b,d,\omega_i>0).$$

Similar to SECR, $\Pr(\omega_i\mid\ b,d,\omega_i>0)=\ \int\Pr(\omega_i\mid\ b,d,\omega_i>0,\boldsymbol{X})f(\boldsymbol{X}\mid b,d,\omega_i>0)$. The resulting distribution of detected animals' home-range centres is

$$f(\boldsymbol{X}|\ b,d,\omega_i>0)=\ p_{\cdot}(\boldsymbol{X}\mid b,d)D(\boldsymbol{X};\tau)/\int(p_{\cdot}(\boldsymbol{X}\mid b,d)D(\boldsymbol{X};\tau)\,d\boldsymbol{X},$$

which results in

$$\Pr(\omega_i\mid\ b,d,\omega_i>0)=$$
$$\int\Pr(\omega_i\mid\ b,d,\omega_i>0,\boldsymbol{X})p_{\cdot}(\boldsymbol{X}\mid b,d)D(\boldsymbol{X};\tau)\,d\boldsymbol{X}/\int p_{\cdot}(\boldsymbol{X}|\ b,d)D(\boldsymbol{X};\tau)d\boldsymbol{X}.$$

As indicated earlier,

$$\Pr(\omega_i \mid b, d, \omega_i > 0, \boldsymbol{X}) = p_{\cdot}(\boldsymbol{X} \mid b, d)^{-1} \prod_{j=b}^{d} \prod_{k=1}^{K_j} \prod_{s=1}^{S_j} {p_{jks}}^{\omega_{ijks}} (1 - p_{jks})^{1-\omega_{ijks}}.$$

Estimates of super-population density can be calculated using the same method used in SECR to calculate time-specific densities. OSECR also has an equivalent to the SECR conditional model: $\mathrm{L}(\theta \mid n, \omega) \propto \prod_{i=1}^{n} \sum_{b=1}^{f_i} \sum_{d=l_i}^{J} \Pr(b, d) \int \frac{\Pr(\omega_i \mid \boldsymbol{X}; \theta, b, d) d\boldsymbol{X}}{\int p_{\cdot}(\boldsymbol{X} \mid b, d)}$, where $\Pr(\omega_i \mid \boldsymbol{X}; \theta, b, d) = \prod_{j=b}^{d} \prod_{k=1}^{K_j} \prod_{s=1}^{S_j} {p_{jks}}^{\omega_{ijks}} (1 - p_{jks})^{1-\omega_{ijks}}$. Note that this model assumes a homogenous distribution of home-range centres. Estimates of superpopulation density using the conditional OSECR model can be found using a Horvtiz-Thompson style estimator, similar to SECR. Similar to JSSA, OSECR can be parameterized in terms of per-capita recruitment (f), either through calculating it recursively as described in the JSSA section of this appendix, or by using the parameterization of Link & Barker (2005) modified for spatial detection in the same vein JSSA was. These models are sometimes referred to as spatial PLB models.

OSECR's model assumptions can be thought of as a mixture of those from JSSA and SECR:

- Detection probabilities are independent between animals.
- Detection probabilities are independent within animals.
- Animals remain individually identifiable throughout the study period.
- Year-to-year survival, and per-capita recruitment are the same for both detected and undetected animals who share the same covariate values. Similarly, detection probability at a given detector is equivalent for animals that have the same covariate values, and home-range centres.
- Animals do not die in the detection process.
- Home-range centres are stationary (this can be relaxed if desired).
- Once an animal has left the population, it cannot return, i.e. animals do not temporarily emigrate (this can be relaxed if home-range centre movement is explicitly modelled).

OSECR models with homogenous density have been implemented in the R programming language, using the package *openCR* (Efford, 2019). As of now, *openCR* does not accommodate inhomogeneous population densities. To ease computation,

openCR treats the study region as a series of equal area discrete pixels in a finite 2-dimensional polygon instead of as $\mathcal{R}^2$. Each pixel contains a point where it is assumed a home-range centre could exist. As a result, all the integrals in the OSECR likelihood are replaced with summations over this set of pixels. For example, the distribution of an animal's home-range centre, conditional on its capture would be $f(x_i \mid b, d, \omega_i > 0) = p_\cdot(x_i \mid b, d) / \sum_{i=1}^{P} p_\cdot(x_i \mid b, d)$, where P is the number of pixels used (note that due to density being assumed homogenous, the Poisson point process terms cancel out). By default *openCR* uses the *nlm* function in R, which employs a Newton-Raphson style algorithm, to maximize this discretized likelihood (R Core Team, 2019).

When fitting an OSECR model with *openCR*, it is important to include a large buffer region of pixels around each detector so that all plausible home-range centre locations are included in the study area that is summed over when calculating marginal detection probabilities. This buffer should be selected so that home-range centres at its outer limits have a detection probability of essentially zero. Failing to account for this can bias parameter estimates. Similarly, it is important to use a grid of pixels that isn't too coarse relative to animal home-range sizes, otherwise this can also bias parameter estimates.

Appendix 2.

Analysis of the South Rockies Grizzly Bear Project Data

Appendix 2.1: South Rockies Grizzly Bear Project Study Design

South Rockies Grizzly Bear Project sampling has been carried out on a yearly basis since 2006, with one primary sampling occasion each year, and multiple secondary occasions within each primary occasion. Both BS, and RO detectors were deployed during the study period.

With the exception of 2012, BS locations were selected by imposing a 14 x 14 km grid over the study area of interest, and placing one BS in each square of this grid. The location of a BS within a grid square was selected, based on expert opinion, to maximize detection success. BS detectors were typically left out for two, 14-day secondary sampling occasions within a year, with hair samples being collected at the end of each occasion. BS detectors were not moved between sessions within a year, and were not deployed in the same location in back-to-back years. After hair samples had been collected from a BS, a blowtorch was used to burn off any lingering hairs from the barbed wire, to prevent them from being mistakenly identified as having been deposited during the subsequent secondary period. This was also done for RO detectors.

RO locations were selected by using expert opinion to determine where bears were most likely to rub. Selected locations were typically trees, fence posts or sign posts that displayed evidence bears were rubbing on them. As the study continued, more and more RO sites were discovered. RO detectors were typically checked every 30 – 40 days during a primary period, however this number could vary substantially (much more than was the case for BS). RO detectors were typically spaced at least 500m apart from one another. RO coverage was sometimes spotty because there were areas where field staff struggled to find suitable trees.

A sample of hair was only subjected to genetic analyses if it contained enough individual hairs to ensure a high probability of successfully identifying which bear it came from (Lamb et al., 2016). In addition, if multiple samples of hair appeared as if they came from the same bear (due to colouration, location on the detector's barbed wire, etc.) then they were marked as such, and once one of them produced a successful identification, the remaining samples were not analyzed. This was done to control costs, and as a result, it is possible that detections were missed because of this.

Table A2.1. Additional details on the sampling carried out each year in the South Rockies Grizzly Bear Project. Trap nights is the sum of the total number of days each detector deployed in a given year was capable of detecting grizzly bears.

Year (Primary Occasion)	Secondary Occasions	Sampling Date Range	Bait Sites	Rub-objects	Trap Nights
2006	3	June 8 - July 28	68	1	1929
2007	3	June 25 - July 26	70	6	1862
2008	2	July 6 - July 29	82	16	2219
2009	3	July 7 - September 25	56	74	3908
2010	4	June 28 - October 29	27	89	7713
2011	3	July 11 - October 20	22	157	12946
2012	5	June 6 - October 18	16	176	17694
2013	5	June 26 - October 13	52	209	16574
2014	5	June 21 - October 19	42	221	23545
2015	5	June 3 - October 30	0	244	31898
2016	6	May 4 - November 9	0	246	29364
2017	5	June 11 - November 1	0	271	31345
2018	6	June 5 - November 6	34	276	34532

Figure A2.1 contains the locations of the detectors deployed each year. As can be seen, the composition of detectors varied noticeably between years. This was because, over time, more RO locations were discovered, and so their numbers increased. In addition, since RO detectors were cheaper and easier to deploy than BS detectors, BS numbers were reduced over time, resulting in them temporarily being phased out from 2015 to 2017. The proportion of the study region covered by deployed detectors also varied from year to year. This was mainly caused by changes in the physical layout of the study region itself (such as stands of trees being lost to logging or fires), changes in the scope of the South Rockies Grizzly Bear Project, and changes in budget.

Table A2.1 contains further details on the sampling that was carried out each year. In this table, “Trap Nights” refers to the cumulative sum of the number of days each deployed detector was capable of detecting an animal. As can be seen, trap nights increased substantially over the course of the study, mainly due to additional RO detectors being added to the study (which almost always had longer sampling windows than BS detectors), and later study years having more secondary sampling occasions. This table also shows that all sampling took place no earlier than May, and no later than December. This date range was selected in part to reduce the amount of population turnover between secondary sampling occasions within a primary sampling occasion. Specifically, sampling start dates were selected to be near or after the end of the grizzly bear hunting season (before the hunt was closed indefinitely in 2018) to reduce human caused mortality between secondary occasions. In addition, sampling ended well before the time of year when cubs are typically birthed (Haroldson, Ternent, Gunther, & Schwartz, 2002), limiting recruitment between secondary occasions.

Figure A2.1. Yearly detector layout in the South Rockies Grizzly Bear Project study region.

Appendix 2.2: Exploratory Data Analysis

Before this paper's simulation study was conducted, it was necessary to first perform an exploratory data analysis to verify that the data in the South Rockies Grizzly Bear Project data set conformed to the assumptions of OSECR, and to gain an understanding of the behaviour of the population being studied.

First, some summary statistics commonly used to summarize CR data were calculated for the subsets of data collected in each year (primary occasion) of the study, as well as over the entire data set. Tables A2.2 – A2.15 below contain these summary statistics. Each table has a column for each secondary occasion within the primary occasion of interest, except for the final table, which contains these summary statistics

for the entire data set. Each row in a table contains a different summary statistic. The first three rows of each table warrant explanation: n refers to the number of bears detected on each occasion, u refers to the number of individuals detected for the first time on a given occasion, and f refers to the number of individuals detected exactly f times.

Table A2.2. Summary statistics for the 2006 South Rockies Grizzly Bear Project data.

2006	1	2	3	Total
n	10	40	53	103
u	10	39	39	88
f	73	15	0	88
detections	10	44	57	111
detectors visited	5	29	38	72
detectors used	6	61	69	136

Table A2.3. Summary statistics for the 2007 South Rockies Grizzly Bear Project data.

2007	1	2	3	Total
n	1	62	40	103
u	1	62	34	97
f	91	6	0	97
detections	1	69	42	112
detectors visited	1	38	29	68
detectors used	1	69	63	133

Table A2.4. Summary statistics for the 2008 South Rockies Grizzly Bear Project data.

2008	1	2	Total
n	31	62	93
u	31	56	87
f	81	6	87
detections	35	64	99
detectors visited	27	40	67
detectors used	68	97	165

Table A2.5. Summary statistics for the 2009 South Rockies Grizzly Bear Project data.

2009	1	2	3	Total
n	57	42	5	104
u	57	30	5	92
f	80	12	0	92
detections	66	47	7	120
detectors visited	32	38	6	76
detectors used	73	95	33	201

Table A2.6. Summary statistics for the 2010 South Rockies Grizzly Bear Project data.

2010	1	2	3	4	Total
n	0	20	41	18	79
u	0	20	33	14	67
f	56	10	1	0	67
detections	0	25	44	18	87
detectors visited	0	20	33	17	70
detectors used	2	47	79	75	203

Table A2.7. Summary statistics for the 2011 South Rockies Grizzly Bear Project data.

2011	1	2	3	Total
n	16	35	43	94
u	16	32	32	80
f	66	14	0	80
detections	16	35	55	106
detectors visited	13	31	46	90
detectors used	56	113	152	321

Table A2.8. Summary statistics for the 2012 South Rockies Grizzly Bear Project data.

2012	1	2	3	4	5	Total
n	17	57	41	43	15	173
u	17	44	19	30	3	113
f	73	26	10	2	2	113
detections	32	82	51	49	21	235
detectors visited	15	57	37	43	15	167
detectors used	18	167	176	179	37	577

Table A2.9. Summary statistics for the 2013 South Rockies Grizzly Bear Project data.

2013	1	2	3	4	5	Total
n	1	31	37	27	35	131
u	1	31	33	20	24	109
f	89	18	2	0	0	109
detections	1	33	42	30	46	152
detectors visited	1	22	31	28	44	126
detectors used	11	103	105	168	185	572

Table A2.10. Summary statistics for the 2014 South Rockies Grizzly Bear Project data.

2014	1	2	3	4	5	Total
n	8	45	56	35	31	175
u	8	43	40	23	14	128
f	92	28	5	3	0	128
detections	11	48	69	45	43	216
detectors visited	10	37	57	41	42	187
detectors used	58	114	191	200	175	738

Table A2.11. Summary statistics for the 2015 South Rockies Grizzly Bear Project data.

2015	1	2	3	4	5	Total
n	8	43	28	52	43	174
u	8	41	16	37	14	116
f	74	28	12	2	0	116
detections	10	50	36	71	63	230
detectors visited	10	42	32	64	57	205
detectors used	48	194	234	235	238	949

Table A2.12. Summary statistics for the 2016 South Rockies Grizzly Bear Project data.

2016	1	2	3	4	5	6	Total
n	1	8	41	49	50	42	191
u	1	7	39	33	26	21	127
f	81	30	14	2	0	0	127
detections	1	10	56	67	63	53	250
detectors visited	1	10	53	59	51	48	222
detectors used	3	55	215	216	215	168	872

Table A2.13. Summary statistics for the 2017 South Rockies Grizzly Bear Project data.

2017	1	2	3	4	5	Total
n	9	53	41	53	62	218
u	9	47	24	33	30	143
f	90	36	13	3	1	143
detections	9	75	58	82	86	310
detectors visited	6	66	57	67	76	272
detectors used	27	238	254	211	241	971

Table A2.14. Summary statistics for the 2018 South Rockies Grizzly Bear Project data.

2018	1	2	3	4	5	6	Total
n	3	76	54	53	57	55	298
u	3	75	40	25	25	15	183
f	104	51	20	8	0	0	183
detections	3	106	59	72	72	75	387
detectors visited	3	88	33	71	67	74	336
detectors used	20	258	63	248	262	264	1115

Table A2.15. Summary statistics for the full South Rockies Grizzly Bear Project data set.

Full Data Set	1	2	3	4	5	6	7	8	9	10	11	12	13	Total
n	88	97	87	92	67	80	113	109	128	116	127	143	183	1430
u	88	71	52	54	32	39	52	50	57	37	29	39	61	661
f	321	149	85	41	28	17	12	6	2	0	0	0	0	661
detections	111	112	99	120	87	106	235	152	216	230	250	310	387	2415
detectors visited	46	52	57	58	50	75	92	99	131	132	145	160	200	1297
detectors used	69	244	246	271	310	76	98	130	116	179	192	261	263	2455

Examining these tables provides some insight into the data. First, sampling effort generally increased with time, with later primary occasions tending to have more secondary occasions than earlier ones. In addition, most bears were detected between 1 and 3 times over the course of the study. Also, the values of u in the full data set table indicate that turnover was likely, as new animals were consistently being detected well into the study. Overall, these tables show no obvious problems with the South Rockies

Grizzly Bear Project data set that would prevent a CR analysis from being conducted with it.

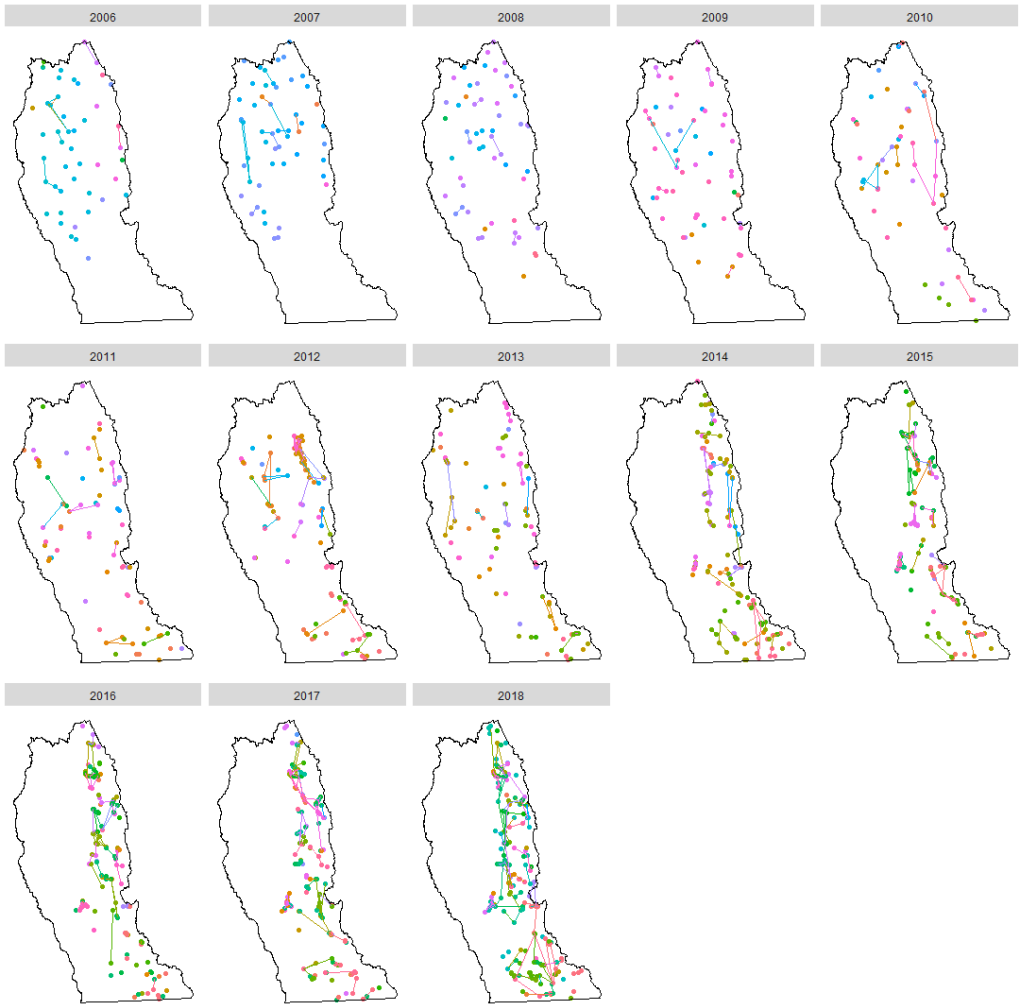

Figure A2.2. Plot of bear recaptures in each year of South Rockies Grizzly Bear Project data. Connected points represent individual recaptures. Bears are individually coloured.

Next, individual detection and redetection data was plotted for each primary occasion (see Figure A2.2). Each individual animal was assigned a unique colour. As can be seen, relative to the scale of the study region, individual detections and redetections typically occurred close to each other. Based on this data it is likely that many animals spend time both within and outside of the study region, thus making it important that an appropriate buffer width is used when analyzing this data set, as well as when simulating spatial CR data. Figure A2.2 seems to indicate that the number of

individuals with multiple detections within a primary period increased over time. This was likely due to secondary occasions and trap nights increasing over the course of the study.

In addition to the CR data collected, several bears were also live-captured and fitted with GPS tracking collars that would transmit, in some cases, multiple locations a day. This telemetry data was analyzed to investigate bear home-range shape, whether home-range centres appear to move between years, and whether the Gaussian space usage model implied by the half-normal detection function appears to be present in the data.

First, telemetry data for a subset of the collared bears was plotted to compare bear movements between years. Specifically, a bear's average location for each day it had location data collected was plotted. This was done because the number of locations transmitted by a collar on a given day could vary drastically. Few bears had the amount of location data necessary for this kind of comparison, and so it was only possible to compare the movements of three bears between years: Bailey, a female bear born in 2012, Brittney, a female bear born in 2011, and Olson, a male bear born in 2009. 2017 and 2018 movement data for these bears can be found in Figure A2.3. It should be noted that only movement data recorded in the same months in both 2017 and 2018 were compared: July – November for Bailey, June – November for Brittney, and May, June, and October for Olson. Yearly home-range centres were estimated by respectively averaging each bear's average daily x, and y coordinates. These are displayed as black points.

Figure A2.3 provides some insights. First, it suggests that the bears in this study have roughly circular home-ranges. It also shows (especially with respect to Olson) that there may be home-range centre movement between years. Table A2.16 contains the distance between estimated home-range centres for each bear.

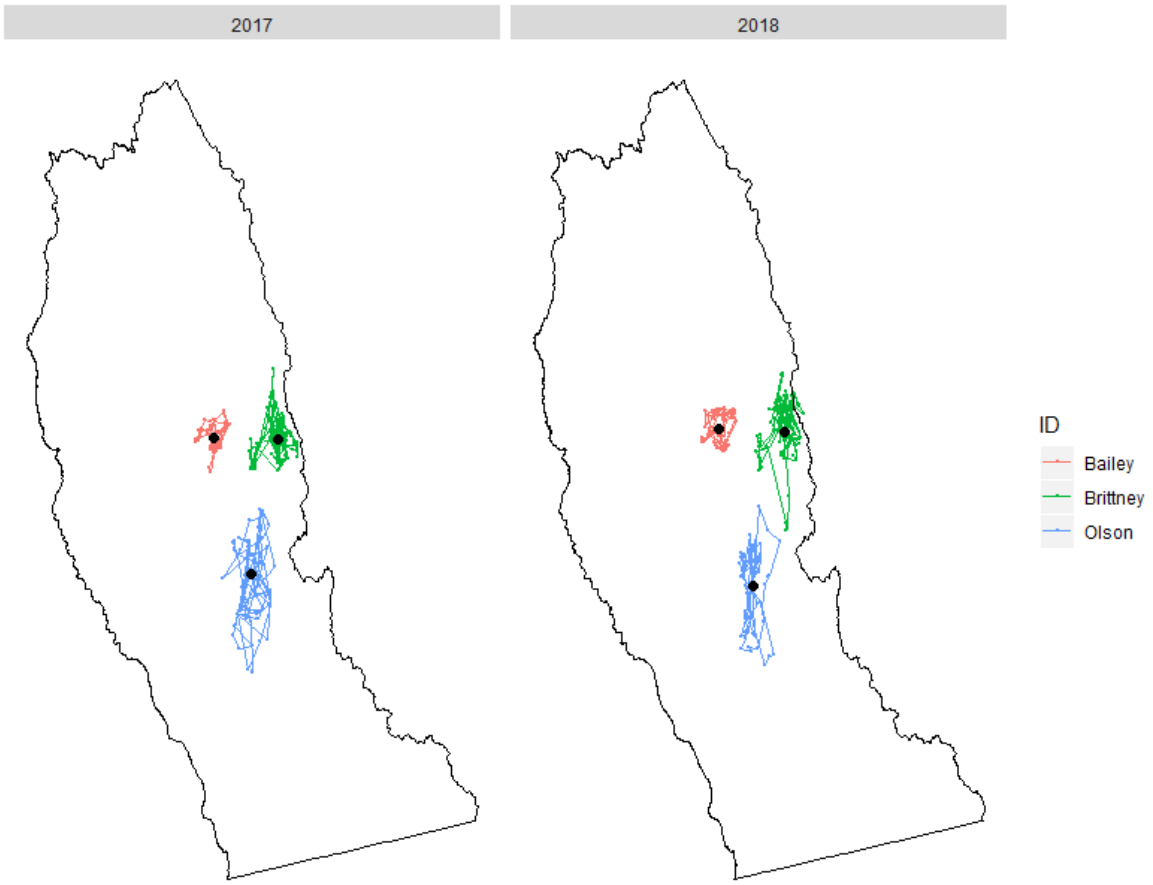

Figure A2.3. Plots of average locations in 2017 and 2018 for South Rockies Grizzly Bear Project bears Bailey, Brittney, and Olson. Average movement data was from July-November for Bailey, June-November for Brittney, and May, June, and October for Olson. Black point mark each bear's estimated home-range centre for a given year, calculated via average the x and y coordinates of each day's average location.

Table A2.16. Euclidian distance between estimated 2017 and 2018 home-range centres for each bear in Figure A2.3.

Bear	Distance between estimated home-range centres (km)
Bailey	2.18
Brittney	1.90
Olson	3.06

It is not surprising that home-range centres appeared to have shifted between 2017 and 2018, as bears may change their space usage patterns over time based on changes in their habitat, and in human disturbance levels, from one year to the next. Too much weight shouldn't be put on the exact observed home-range shapes, and calculated

movements in home-range centres, as only 3 bears had sufficient data for analysis, and the data available only covered a portion of each year.

Finally, individual telemetry data was examined to see if the collared bears appeared to follow a Gaussian space usage pattern. For this to be the case, space usage probabilities should resemble those of a circular bivariate Gaussian distribution, with mean equivalent to the animal's home-range centre.

Upon analyzing telemetry data from several bears, it did not appear that bears followed this space usage pattern. Figure A2.4 contains the movements for a 16-year-old bear named Gums. Location data for Gums was collected daily between May 2018 and October 2018. On most days, four locations were collected at times 00:00, 06:00, 12:00, and 18:00. There were some instances where only two or three locations were collected on a given day, but this happened rarely. Points with the same colour were collected on the same day. Gums' estimated home-range centre is marked as a black point.

As can be seen, there are multiple areas a large distance away from the home-range centre, relative to the observed home-range size, that have high usage. This goes against the Gaussian space usage assumption that space usage would monotonically decrease with distance from the home-range centre. This is not surprising, and there are many reasons why a bear would act in such a manner, such as discovering a region abundant in food that it wishes to stay in. These general findings were observed in essentially all of the collared bears that had enough data available to properly analyze. Efford (2014) details how the SECR detection function can be modified to account for space usage caused by resource selection, and this could potentially be extended to an OSECR fit to South Rockies Grizzly Bear Project data. However, it does not seem that the *openCR* package is currently equipped to make this adjustment. As such, the space usage assumption will likely be violated when fitting OSECR models to the South Rockies Grizzly Bear Project data set. Ideally the OSECR model will be robust to this violation, however we are unsure if this will be the case. Data used in the simulation study portion of this paper were generated assuming space usage conforms to the assumptions of OSECR for simplicity's sake.

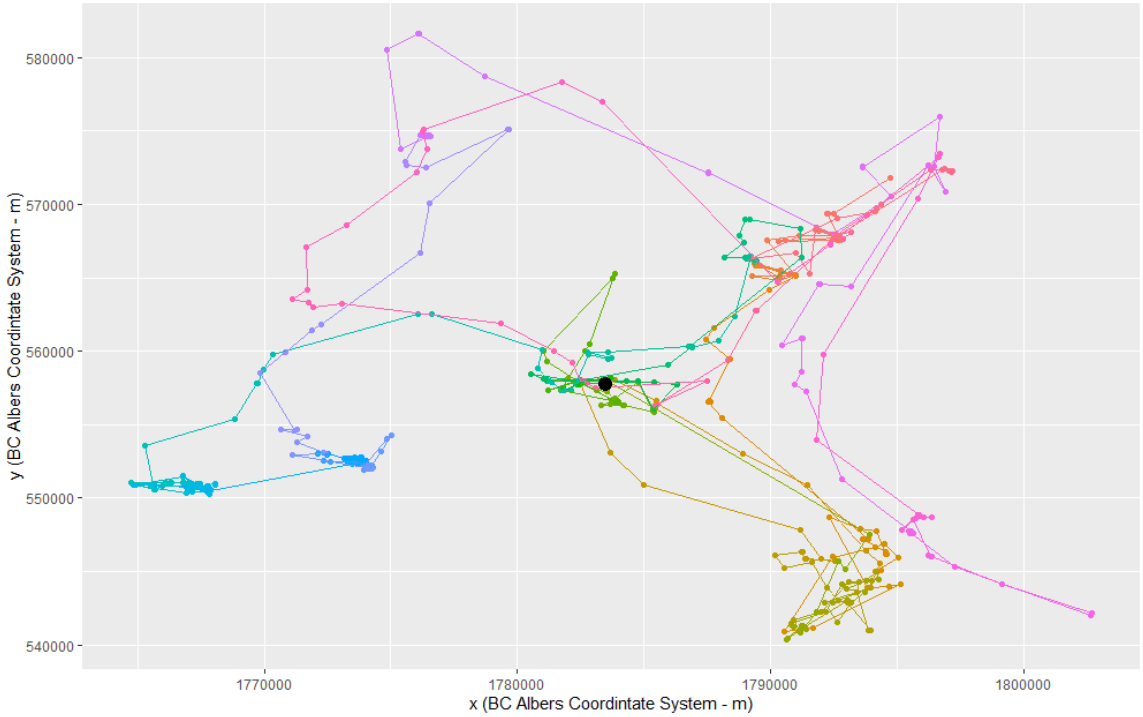

Figure A2.4. Movement data for a South Rockies Grizzly Bear Project bear names Gums, taken between May-October 2018. Each day is individually coloured, with dates close together being similarly coloured (multiple locations were recorded each day). In black is the estimated home-range centre calculated by taking the average of the recorded x and y coordinates.

Appendix 3.

Additional Figures and Tables

Appendix 3.1: Additional Figures

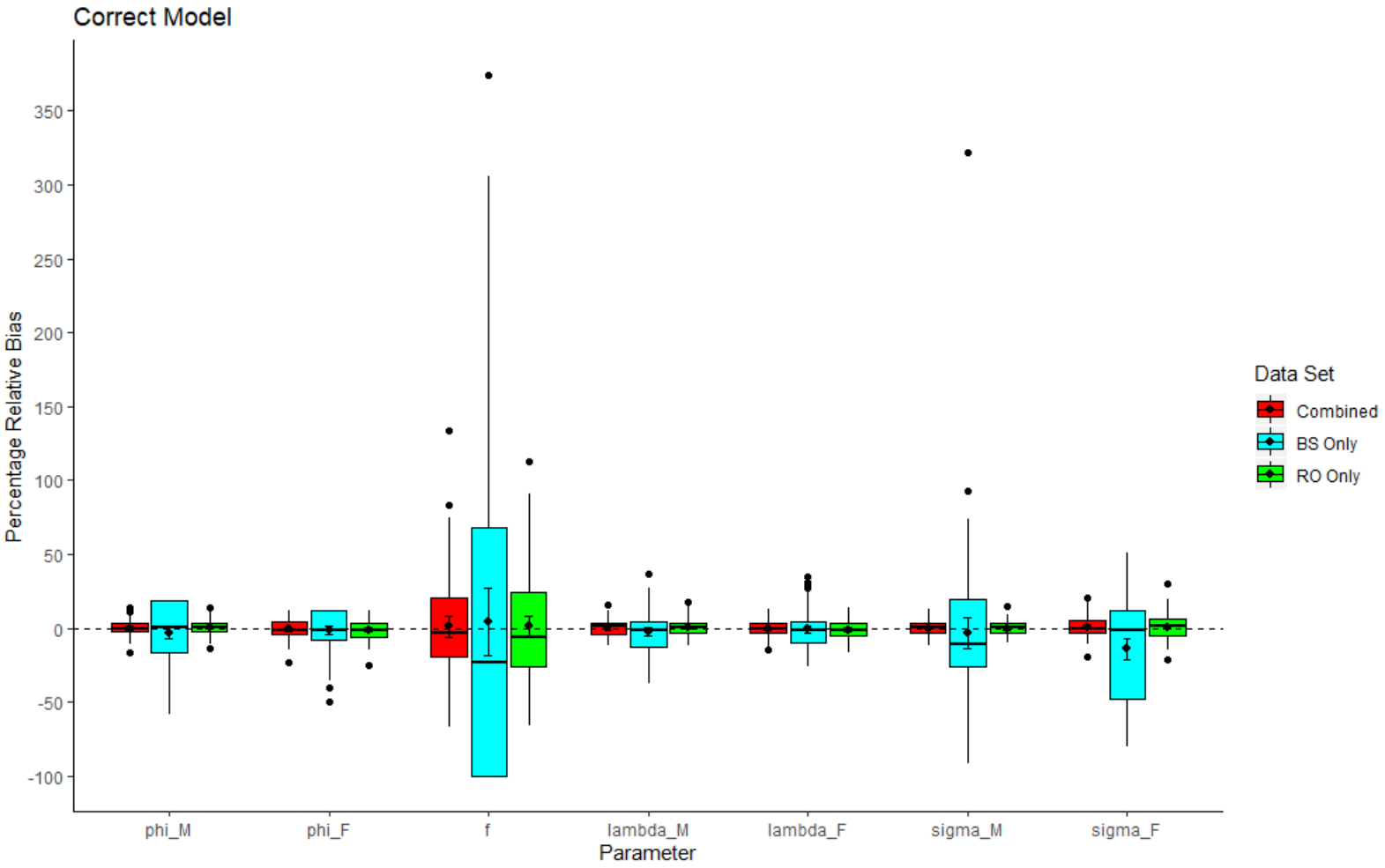

Figure A3.1. Standard boxplots of the percentage relative bias for each parameter of interest in M_c for the λ_0 – Small simulated scenario. Whiskers extend a distance of 1.5 time the inter-quartile range from the median. Sample mean biases along with corresponding 95% confidence intervals are also included. This figure contains the same M_c data found in Figures 3.1 – 3.3, rearranged to aid comparisons between simulated data sets.

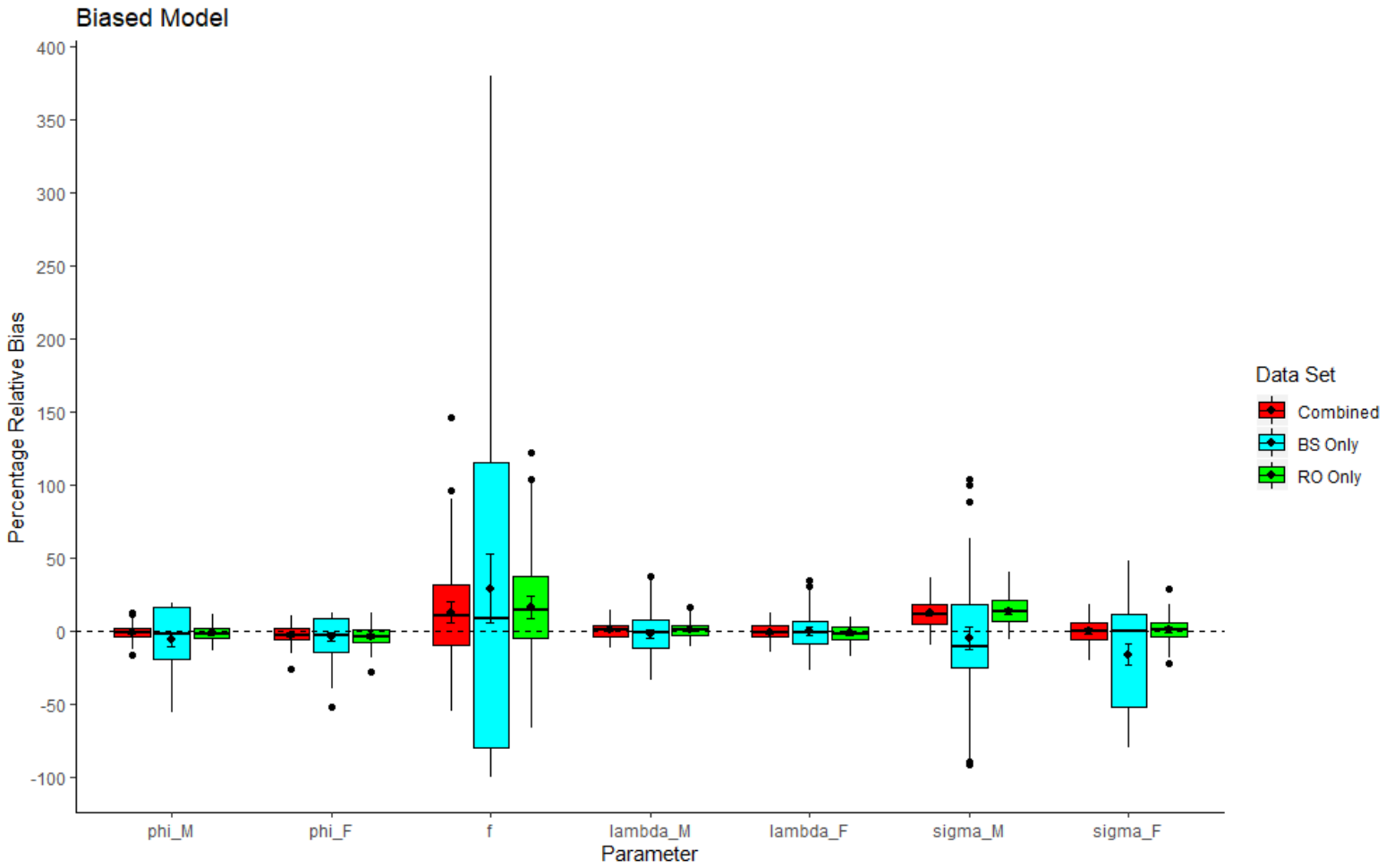

Figure A3.2. Standard boxplots of the percentage relative bias for each parameter of interest in M_b for the λ_0 – Small simulated scenario. Whiskers extend a distance of 1.5 time the inter-quartile range from the median. Sample mean biases along with corresponding 95% confidence intervals are also included. This figure contains the same M_b data found in Figures 3.1 – 3.3, rearranged to aid comparisons between simulated data sets

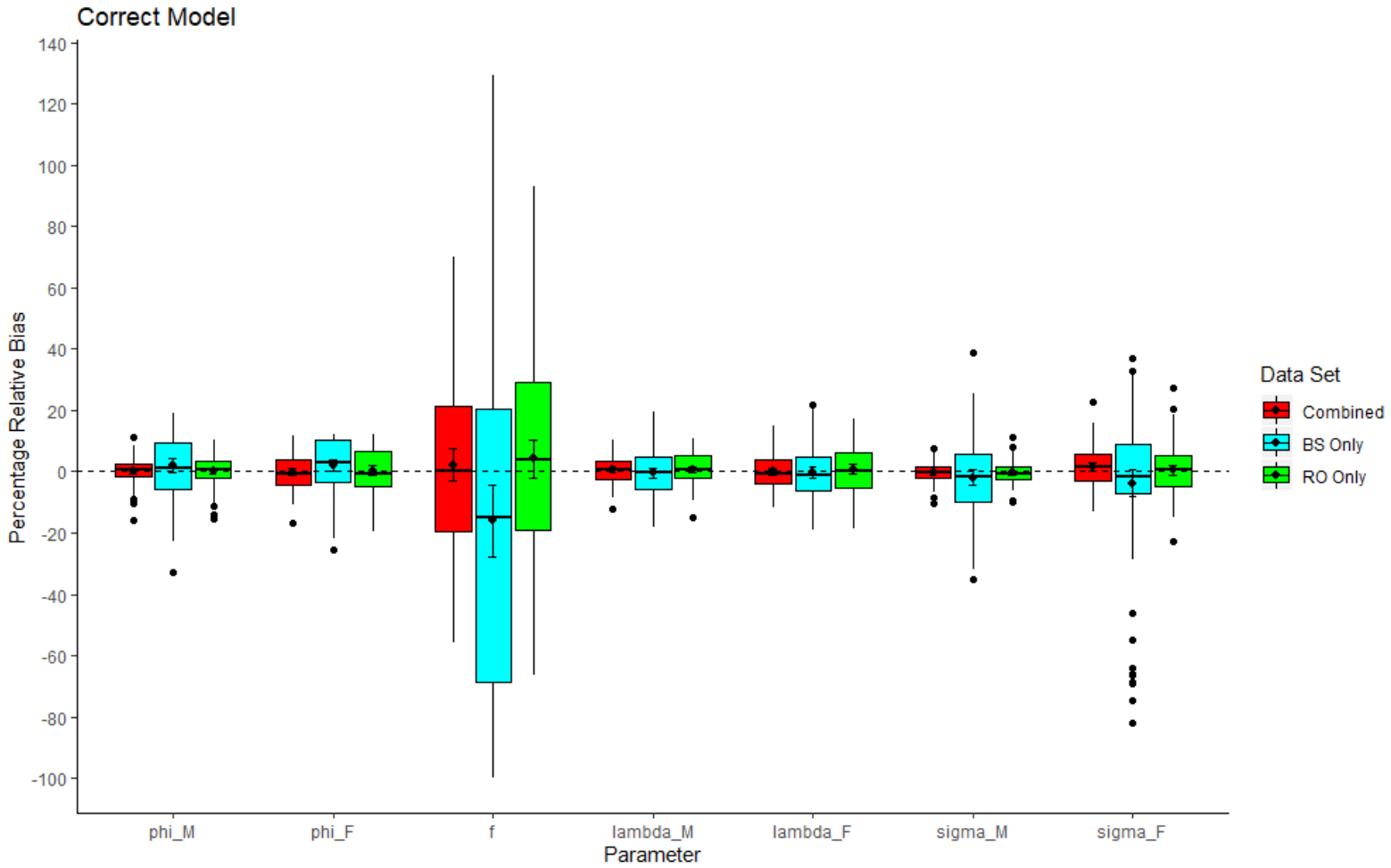

Figure A3.3. Standard boxplots of the percentage relative bias for each parameter of interest in M_c for the λ_0 – Moderate simulated scenario. Whiskers extend a distance of 1.5 time the inter-quartile range from the median. Sample mean biases along with corresponding 95% confidence intervals are also included. This figure contains the same M_c data found in Figures 3.4 – 3.6, rearranged to aid comparisons between simulated data sets.

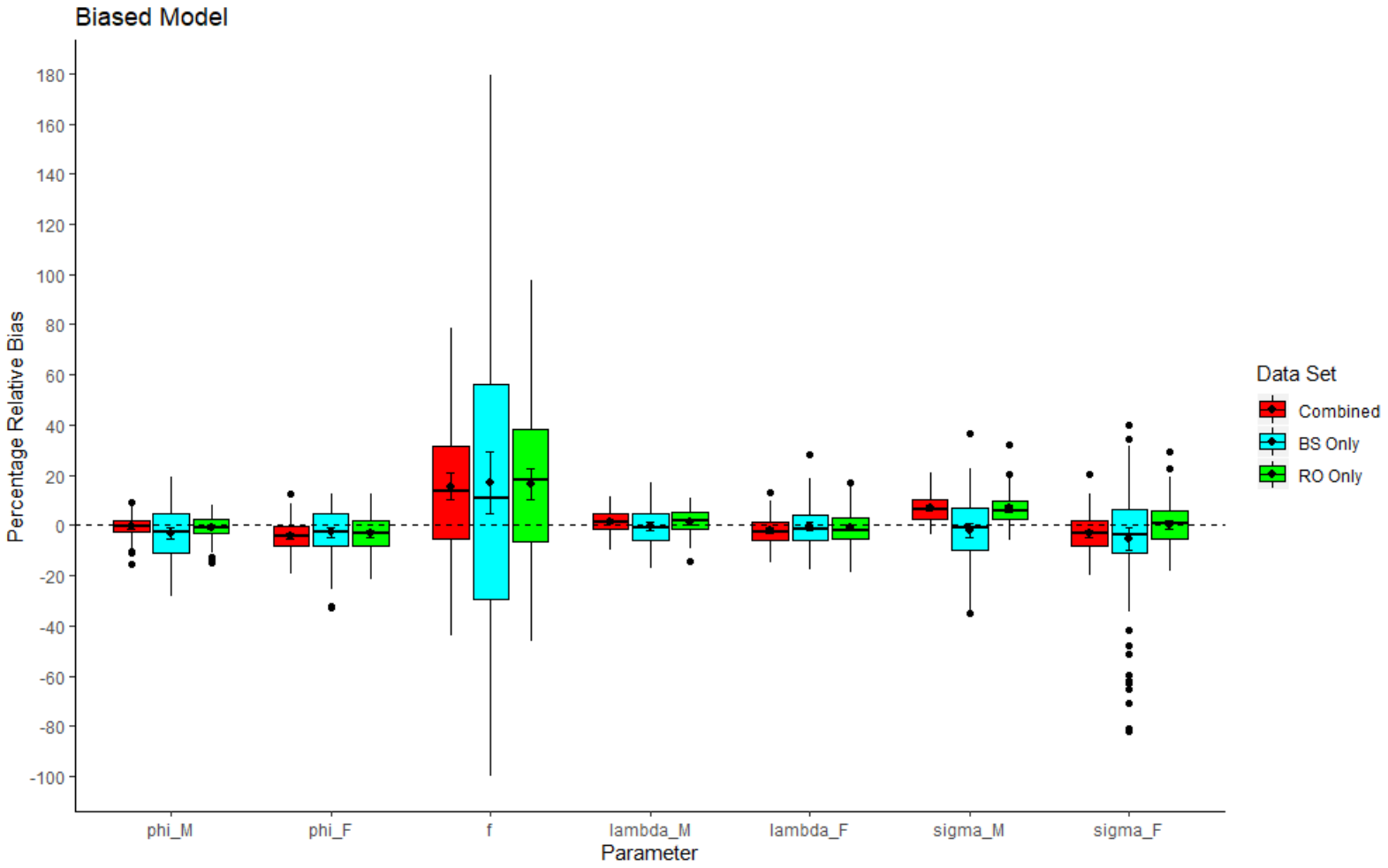

Figure A3.4. Standard boxplots of the percentage relative bias for each parameter of interest in M_b for the λ_0 – Moderate simulated scenario. Whiskers extend a distance of 1.5 time the inter-quartile range from the median. Sample mean biases along with corresponding 95% confidence intervals are also included. This figure contains the same M_b data found in Figures 3.4 – 3.6, rearranged to aid comparisons between simulated data sets.

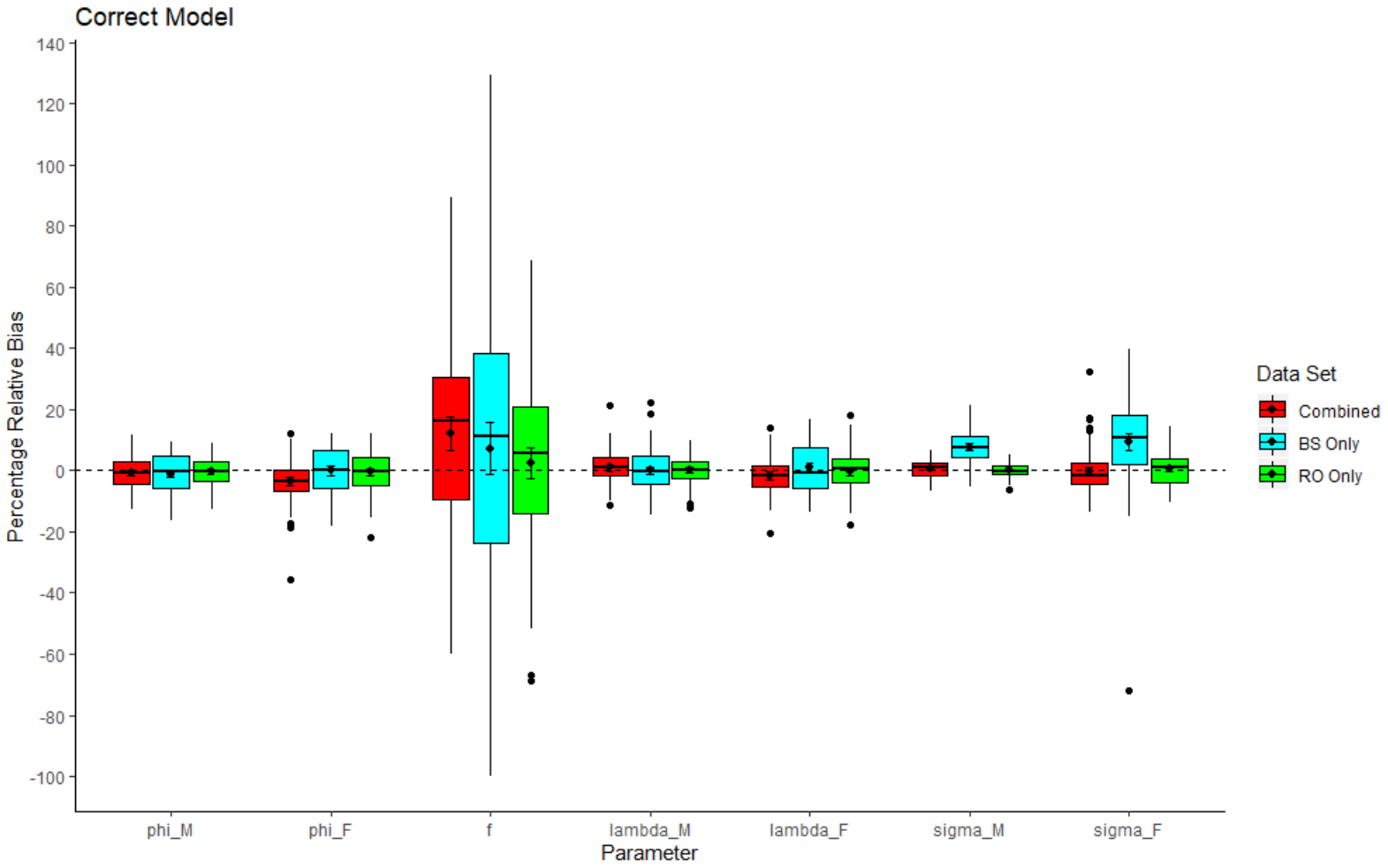

Figure A3.5. Standard boxplots of the percentage relative bias for each parameter of interest in M_c for the λ_0 – Large simulated scenario. Whiskers extend a distance of 1.5 time the inter-quartile range from the median. Sample mean biases along with corresponding 95% confidence intervals are also included. This figure contains the same M_c data found in Figures 3.7 – 3.9, rearranged to aid comparisons between simulated data sets.

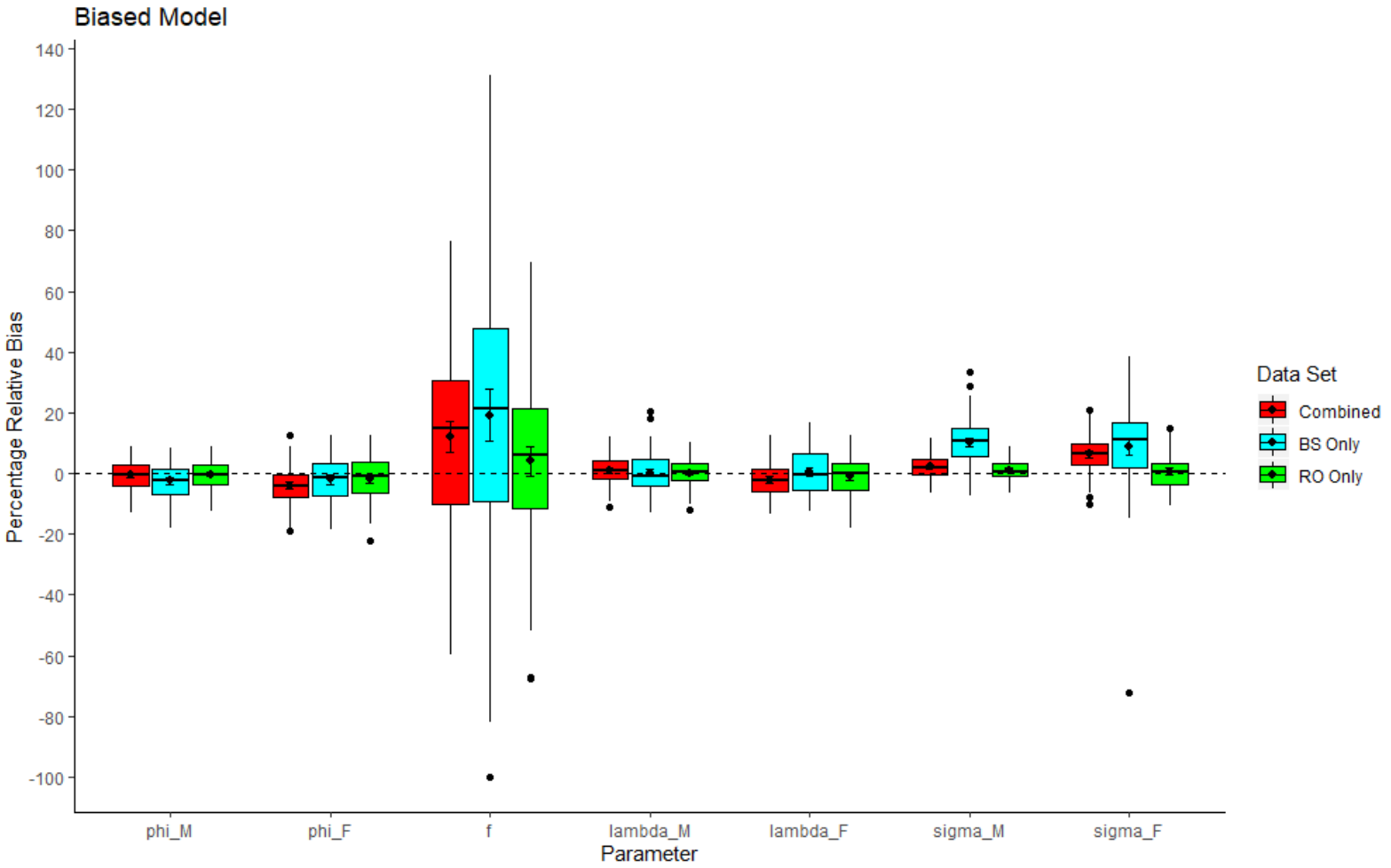

Figure A3.6. Standard boxplots of the percentage relative bias for each parameter of interest in M_b for the λ_0 – Large simulated scenario. Whiskers extend a distance of 1.5 time the inter-quartile range from the median. Sample mean biases along with corresponding 95% confidence intervals are also included. This figure contains the same M_b data found in Figures 3.7 – 3.9, rearranged to aid comparisons between simulated data sets.

Appendix 3.2: Additional Tables

Table A3.1. Summary statistics for the percentage relative biases observed in each parameter of interest, in the λ_0 – Small simulated scenario using the full simulated data set.

Model	Parameter	Mean % Relative Bias	Mean % Relative Bias Lower 95% CL	Mean % Relative Bias Upper 95% CL	Median % Relative Bias	% Relative Bias Quartile 1	% Relative Bias Quartile 3
Correct	ϕ_{Males}	0.22	-0.82	1.26	0.09	-2.37	3.16
Correct	$\phi_{Females}$	-0.49	-1.78	0.80	-0.76	-3.70	4.16
Correct	f	1.20	-5.59	8.00	-3.29	-19.55	20.33
Correct	λ_{Males}	0.34	-0.76	1.45	1.24	-4.18	3.60
Correct	$\lambda_{Females}$	-0.29	-1.38	0.81	-0.51	-3.54	3.36
Correct	σ_{Males}	0.19	-0.71	1.09	0.57	-2.99	3.40
Correct	$\sigma_{Females}$	0.75	-0.64	2.14	0.22	-3.40	5.29
Biased	ϕ_{Males}	-1.08	-2.16	0.00	-1.08	-4.27	1.67
Biased	$\phi_{Females}$	-2.49	-3.74	-1.23	-2.64	-5.99	1.64
Biased	f	12.78	5.88	19.67	10.64	-9.30	31.53
Biased	λ_{Males}	0.65	-0.44	1.74	1.05	-4.11	4.22
Biased	$\lambda_{Females}$	-0.67	-1.72	0.38	-1.04	-4.05	3.33
Biased	σ_{Males}	11.97	10.14	13.81	11.84	5.00	18.20
Biased	$\sigma_{Females}$	-0.11	-1.60	1.39	-0.10	-5.54	5.38

Table A3.2. Summary statistics for the percentage relative biases observed in each parameter of interest, in the λ_0 – Small simulated scenario using the BS only data set.

Model	Parameter	Mean % Relative Bias	Mean % Relative Bias Lower 95% CL	Mean % Relative Bias Upper 95% CL	Median % Relative Bias	% Relative Bias Quartile 1	% Relative Bias Quartile 3
Correct	ϕ_{Males}	-3.17	-7.32	0.98	0.44	-16.85	19.04
Correct	$\phi_{Females}$	-1.17	-3.89	1.54	-0.73	-8.30	12.35
Correct	f	4.21	-18.70	27.13	-23.50	-100.00	67.74
Correct	λ_{Males}	-2.25	-5.27	0.78	-1.01	-12.86	4.77
Correct	$\lambda_{Females}$	-0.53	-3.08	2.02	-0.99	-9.34	4.63
Correct	σ_{Males}	-3.17	-13.33	6.98	-11.02	-26.16	19.76
Correct	$\sigma_{Females}$	-13.90	-20.99	-6.82	-0.73	-47.38	12.44
Biased	ϕ_{Males}	-6.07	-10.34	-1.80	-2.00	-19.66	16.12
Biased	$\phi_{Females}$	-4.15	-6.95	-1.34	-3.09	-14.24	8.26
Biased	f	28.94	5.45	52.43	8.85	-79.43	115.32
Biased	λ_{Males}	-1.69	-4.67	1.28	-1.21	-11.65	7.67
Biased	$\lambda_{Females}$	-0.22	-2.86	2.43	-1.34	-8.94	6.39
Biased	σ_{Males}	-4.66	-12.38	3.06	-10.63	-24.70	18.51
Biased	$\sigma_{Females}$	-16.08	-23.58	-8.57	-0.28	-52.20	11.23

Table A3.3. Summary statistics for the percentage relative biases observed in each parameter of interest, in the λ_0 – Small simulated scenario using the RO only data set.

Model	Parameter	Mean % Relative Bias	Mean % Relative Bias Lower 95% CL	Mean % Relative Bias Upper 95% CL	Median % Relative Bias	% Relative Bias Quartile 1	% Relative Bias Quartile 3
Correct	ϕ_{Males}	0.39	-0.65	1.43	0.28	-2.53	3.53
Correct	$\phi_{Females}$	-1.11	-2.56	0.34	-1.24	-5.51	3.25
Correct	f	1.34	-5.97	8.64	-6.14	-26.23	24.33
Correct	λ_{Males}	0.51	-0.64	1.65	1.09	-3.39	3.83
Correct	$\lambda_{Females}$	-0.82	-2.01	0.37	-1.21	-5.07	3.85
Correct	σ_{Males}	0.09	-0.84	1.02	0.28	-3.57	3.18
Correct	$\sigma_{Females}$	0.98	-0.67	2.63	1.49	-4.61	6.02
Biased	ϕ_{Males}	-1.43	-2.50	-0.36	-1.53	-4.98	1.94
Biased	$\phi_{Females}$	-3.81	-5.25	-2.36	-3.75	-7.72	1.01
Biased	f	16.33	8.97	23.69	13.98	-5.34	37.39
Biased	λ_{Males}	0.79	-0.31	1.90	1.13	-3.15	4.04
Biased	$\lambda_{Females}$	-1.41	-2.58	-0.24	-1.63	-5.57	3.25
Biased	σ_{Males}	13.49	11.51	15.48	13.74	6.23	20.80
Biased	$\sigma_{Females}$	0.89	-0.80	2.58	1.38	-4.09	5.94

Table A3.4. Summary statistics for the percentage relative biases observed in each parameter of interest, in the λ_0 – Moderate simulated scenario using the full simulated data set.

Model	Parameter	Mean % Relative Bias	Mean % Relative Bias Lower 95% CL	Mean % Relative Bias Upper 95% CL	Median % Relative Bias	% Relative Bias Quartile 1	% Relative Bias Quartile 3
Correct	ϕ_{Males}	0.25	-0.62	1.12	0.66	-1.70	2.66
Correct	$\phi_{Females}$	-0.19	-1.34	0.96	-0.57	-4.15	4.05
Correct	f	2.27	-2.99	7.54	0.39	-19.57	21.55
Correct	λ_{Males}	0.50	-0.37	1.38	0.48	-2.69	3.67
Correct	$\lambda_{Females}$	0.10	-1.01	1.21	-0.47	-3.84	4.10
Correct	σ_{Males}	-0.30	-0.96	0.36	-0.33	-2.19	1.61
Correct	$\sigma_{Females}$	1.69	0.38	3.00	1.83	-2.85	5.89
Biased	ϕ_{Males}	-0.58	-1.46	0.29	-0.15	-2.83	2.07
Biased	$\phi_{Females}$	-4.24	-5.39	-3.08	-4.43	-8.42	-0.18
Biased	f	15.38	10.00	20.75	13.84	-5.51	31.51
Biased	λ_{Males}	1.41	0.55	2.27	1.50	-1.53	4.45
Biased	$\lambda_{Females}$	-1.91	-3.00	-0.81	-2.32	-5.95	1.48
Biased	σ_{Males}	6.90	5.78	8.01	6.36	2.70	10.53
Biased	$\sigma_{Females}$	-3.24	-4.70	-1.77	-3.33	-8.21	1.92

Table A3.5. Summary statistics for the percentage relative biases observed in each parameter of interest, in the λ_0 – Moderate simulated scenario using the BS only data set.

Model	Parameter	Mean % Relative Bias	Mean % Relative Bias Lower 95% CL	Mean % Relative Bias Upper 95% CL	Median % Relative Bias	% Relative Bias Quartile 1	% Relative Bias Quartile 3
Correct	ϕ_{Males}	1.94	-0.27	4.15	0.95	-5.85	9.58
Correct	$\phi_{Females}$	1.95	0.19	3.71	3.15	-3.53	10.47
Correct	f	-16.09	-27.98	-4.20	-14.79	-68.90	20.56
Correct	λ_{Males}	-0.31	-1.89	1.26	-0.22	-5.87	4.93
Correct	$\lambda_{Females}$	-0.19	-1.84	1.45	-0.99	-6.30	4.72
Correct	σ_{Males}	-1.89	-4.58	0.80	-1.81	-10.10	5.68
Correct	$\sigma_{Females}$	-3.71	-8.20	0.78	-1.43	-6.99	8.76
Biased	ϕ_{Males}	-3.01	-5.14	-0.88	-2.83	-10.72	4.66
Biased	$\phi_{Females}$	-2.84	-4.80	-0.88	-2.67	-8.18	4.53
Biased	f	17.07	4.65	29.49	11.06	-29.21	56.05
Biased	λ_{Males}	-0.50	-2.06	1.07	-0.85	-6.09	4.83
Biased	$\lambda_{Females}$	-0.48	-2.18	1.23	-1.26	-6.18	4.35
Biased	σ_{Males}	-1.87	-4.57	0.82	-0.89	-9.76	6.77
Biased	$\sigma_{Females}$	-5.50	-9.99	-1.01	-3.60	-10.81	6.64

Table A3.6. Summary statistics for the percentage relative biases observed in each parameter of interest, in the λ_0 – Moderate simulated scenario using the RO only data set.

Model	Parameter	Mean % Relative Bias	Mean % Relative Bias Lower 95% CL	Mean % Relative Bias Upper 95% CL	Median % Relative Bias	% Relative Bias Quartile 1	% Relative Bias Quartile 3
Correct	ϕ_{Males}	0.32	-0.66	1.30	0.46	-2.26	3.55
Correct	$\phi_{Females}$	0.38	-1.23	1.99	-0.87	-4.94	6.67
Correct	f	4.33	-1.88	10.54	3.78	-19.18	29.34
Correct	λ_{Males}	0.82	-0.19	1.83	0.50	-2.27	5.20
Correct	$\lambda_{Females}$	0.85	-0.64	2.34	0.14	-5.17	6.22
Correct	σ_{Males}	-0.35	-1.07	0.38	-0.67	-2.62	1.57
Correct	$\sigma_{Females}$	0.53	-1.10	2.15	0.71	-4.81	5.26
Biased	ϕ_{Males}	-0.78	-1.74	0.17	-0.75	-3.03	2.72
Biased	$\phi_{Females}$	-3.29	-4.71	-1.86	-3.19	-7.97	1.89
Biased	f	16.57	10.28	22.87	17.91	-6.74	38.21
Biased	λ_{Males}	1.39	0.42	2.36	1.82	-1.68	5.33
Biased	$\lambda_{Females}$	-0.93	-2.28	0.43	-1.96	-5.57	3.25
Biased	σ_{Males}	6.65	5.42	7.89	5.98	2.67	9.74
Biased	$\sigma_{Females}$	0.28	-1.44	2.00	0.93	-5.28	5.63

Table A3.7. Summary statistics for the percentage relative biases observed in each parameter of interest, in the λ_0 – Large simulated scenario using the full simulated data set.

Model	Parameter	Mean % Relative Bias	Mean % Relative Bias Lower 95% CL	Mean % Relative Bias Upper 95% CL	Median % Relative Bias	% Relative Bias Quartile 1	% Relative Bias Quartile 3
Correct	ϕ_{Males}	-0.57	-1.44	0.30	-0.55	-4.19	2.79
Correct	$\phi_{Females}$	-3.46	-4.80	-2.13	-3.27	-6.53	0.37
Correct	f	12.15	6.73	17.57	16.17	-9.21	30.39
Correct	λ_{Males}	1.02	-0.02	2.06	1.03	-1.61	4.32
Correct	$\lambda_{Females}$	-1.61	-2.79	-0.43	-1.43	-5.33	1.52
Correct	σ_{Males}	0.88	0.32	1.44	0.97	-1.49	2.71
Correct	$\sigma_{Females}$	-0.14	-1.48	1.19	-1.60	-4.24	2.58
Biased	ϕ_{Males}	-0.61	-1.43	0.22	-0.40	-4.05	2.65
Biased	$\phi_{Females}$	-3.97	-5.19	-2.74	-4.10	-7.64	-0.22
Biased	f	12.12	7.03	17.21	14.67	-9.95	30.53
Biased	λ_{Males}	0.98	0.04	1.93	0.85	-1.58	4.22
Biased	$\lambda_{Females}$	-2.06	-3.20	-0.91	-2.47	-6.04	1.46
Biased	σ_{Males}	2.35	1.64	3.05	1.81	-0.38	4.80
Biased	$\sigma_{Females}$	6.41	5.29	7.54	6.67	2.90	9.92

Table A3.8. Summary statistics for the percentage relative biases observed in each parameter of interest, in the λ_0 – Large simulated scenario using the BS only data set.

Model	Parameter	Mean % Relative Bias	Mean % Relative Bias Lower 95% CL	Mean % Relative Bias Upper 95% CL	Median % Relative Bias	% Relative Bias Quartile 1	% Relative Bias Quartile 3
Correct	ϕ_{Males}	-0.99	-2.22	0.23	-0.27	-5.89	4.61
Correct	$\phi_{Females}$	0.14	-1.53	1.80	-0.01	-5.96	6.62
Correct	f	7.22	-1.28	15.72	11.42	-23.79	38.50
Correct	λ_{Males}	0.03	-1.23	1.30	-0.33	-4.28	4.65
Correct	$\lambda_{Females}$	0.98	-0.59	2.55	-0.48	-5.62	7.39
Correct	σ_{Males}	7.73	6.73	8.74	7.59	4.20	11.38
Correct	$\sigma_{Females}$	9.34	6.69	11.98	10.89	2.17	17.95
Biased	ϕ_{Males}	-2.42	-3.64	-1.20	-2.07	-7.09	1.69
Biased	$\phi_{Females}$	-1.95	-3.50	-0.39	-1.30	-7.23	3.30
Biased	f	19.17	10.70	27.65	21.38	-9.37	47.93
Biased	λ_{Males}	0.28	-0.92	1.47	-0.68	-3.93	4.50
Biased	$\lambda_{Females}$	0.56	-0.94	2.06	-0.56	-5.46	6.40
Biased	σ_{Males}	10.23	8.73	11.73	10.70	5.43	14.81
Biased	$\sigma_{Females}$	8.86	6.27	11.46	11.28	2.13	16.91

Table A3.9. Summary statistics for the percentage relative biases observed in each parameter of interest, in the λ_0 – Large simulated scenario using the RO only data set.

Model	Parameter	Mean % Relative Bias	Mean % Relative Bias Lower 95% CL	Mean % Relative Bias Upper 95% CL	Median % Relative Bias	% Relative Bias Quartile 1	% Relative Bias Quartile 3
Correct	ϕ_{Males}	-0.22	-1.03	0.59	-0.27	-3.44	2.92
Correct	$\phi_{Females}$	-0.46	-1.83	0.90	-0.21	-4.66	4.58
Correct	f	2.42	-2.57	7.41	5.61	-14.13	20.87
Correct	λ_{Males}	0.11	-0.80	1.02	0.08	-2.43	3.10
Correct	$\lambda_{Females}$	-0.12	-1.42	1.18	0.51	-3.97	3.78
Correct	σ_{Males}	0.03	-0.40	0.46	-0.09	-1.23	1.69
Correct	$\sigma_{Females}$	0.68	-0.47	1.82	1.09	-4.00	3.97
Biased	ϕ_{Males}	-0.24	-1.05	0.56	-0.27	-3.52	2.99
Biased	$\phi_{Females}$	-1.62	-2.98	-0.27	-1.07	-6.24	3.55
Biased	f	4.04	-0.92	9.01	6.30	-11.67	21.31
Biased	λ_{Males}	0.29	-0.61	1.20	0.55	-2.21	3.36
Biased	$\lambda_{Females}$	-0.95	-2.22	0.32	-0.02	-5.58	3.15
Biased	σ_{Males}	1.07	0.44	1.70	0.66	-0.99	3.11
Biased	$\sigma_{Females}$	0.68	-0.45	1.80	0.68	-3.80	3.54

Table A3.10. Parameter estimates for the 4 rounds of simulations in the λ_0 – Small simulated scenario that produced major $\hat{\sigma}_{Males}$ outliers.

$\hat{\phi}_{Males}$	$\hat{\phi}_{Females}$	$\hat{f}$	$\hat{\lambda}_{Males}$	$\hat{\lambda}_{Females}$	$\hat{\sigma}_{Males}$	$\hat{\sigma}_{Females}$	Data Set	Model
0.537	0.536	0.487	1.024	1.023	2.45916E+13	747.447	BS Only	Correct
0.543	0.540	0.484	1.027	1.024	79808725.49	760.421	BS Only	Biased
0.864	1.000	0.220	1.085	1.220	1751885828	4237.451	BS Only	Correct
0.776	0.992	0.257	1.033	1.249	16463614.29	4423.344	BS Only	Biased